Atmos. Chem. Phys. Discuss., doi:10.5194/acp-2017-6, 2017
Manuscript under review for journal Atmos. Chem. Phys.
Published: 11 January 2017

Atmospheric Chemistry and Physics Discussions

Global-scale combustion sources of organic aerosols: Sensitivity to formation and removal mechanisms

Alexandra P. Tsimpidi[1], Vlassis A. Karydis[1], Spyros N. Pandis[2, 3]and Jos Lelieveld[1, 4]

[1] Max Planck Institute for Chemistry, Mainz, Germany
[2] Department of Chemical Engineering, University of Patras, Patras, Greece
[3] Department of Chemical Engineering, Carnegie Mellon University, Pittsburgh, PA, USA
[4] Energy, Environment and Water Research Center, Cyprus Institute, Nicosia, Cyprus
*Corresponding author e-mail: a.tsimpidi@mpic.de

Atmos. Chem. Phys. Discuss., doi:10.5194/acp-2017-6, 2017
Manuscript under review for journal Atmos. Chem. Phys.
Published: 11 January 2017

Atmospheric Chemistry and Physics Discussions

Abstract

Organic compounds from combustion sources such as biomass burning and fossil fuel use are major contributors to the global atmospheric load of aerosols. We analyzed the sensitivity of model-predicted global-scale organic aerosols (OA) to parameters that control primary emissions, photochemical aging and the scavenging efficiency of organic vapors. We used a computationally efficient module for the description of OA composition and evolution in the atmosphere (ORACLE) of the global chemistry-climate model EMAC. A global dataset of aerosol mass spectrometer measurements was used to evaluate simulated primary (POA) and secondary OA (SOA) concentrations. Model results are sensitive to the emission rates of intermediate volatility organic compounds (IVOCs) and POA. Assuming enhanced reactivity of semi-volatile organic compounds (SVOCs) and IVOCs with OH substantially improved the model performance for SOA. Use of a hybrid approach for the parameterization of the aging of IVOCs had a small effect on predicted SOA levels. The model performance improved by assuming that freshly emitted organic compounds are relatively hydrophobic and become increasingly hygroscopic due to oxidation.

1 Introduction

Organic aerosol (OA) is an important constituent of the atmosphere, contributing 30-70% of the total submicron dry aerosol mass (Kanakidou et al., 2005) with major impacts on human health and climate (IPCC, 2013; Lelieveld et al., 2015). OA comprises a large number of compounds with a wide range in volatility and oxidation states. The material that is in the particulate phase upon emission is called primary organic aerosol (POA). The co-emitted organic vapors can undergo one or more chemical transformations, which can reduce their volatility, leading to their transfer to the particulate phase forming secondary organic aerosol (SOA).

Several regional-scale modeling studies have accounted for the semi-volatile nature and chemical aging of organic compounds by using the volatility based set (VBS) approach (Donahue et al., 2006), demonstrating improvements in the accuracy of the predicted concentrations of organic aerosols (OA) and their chemical properties (Robinson et al., 2007; Shrivastava et al., 2008; Murphy and Pandis, 2009; Hodzic et al., 2010; Tsimpidi et al., 2010; Fountoukis et al., 2011; Li et al., 2011; Tsimpidi et

Atmos. Chem. Phys. Discuss., doi:10.5194/acp-2017-6, 2017
Manuscript under review for journal Atmos. Chem. Phys.
Published: 11 January 2017

Atmospheric Chemistry and Physics Discussions

al., 2011; Bergstrom et al., 2012; Athanasopoulou et al., 2013; Zhang et al., 2013; Fountoukis et al., 2014). However, only few global modeling studies have adopted the VBS approach (Pye and Seinfeld, 2010; Jathar et al., 2011; Tsimpidi et al., 2014). According to these studies, the modeled global tropospheric burden of POA is 0.03-0.23 Tg and of SOA 1.61-2.77 Tg, with SVOCs and IVOCs contributing 0.71-1.57 Tg to the total.

The VBS approach is a flexible framework for simulating OA formation and removal; however, there are several uncertainties in the parameters used. The first source of uncertainty is related to the emissions of organic particles and vapors (Kanakidou et al., 2005). The volatility distribution of the fresh POA is important in the VBS as it determines the initial evaporation of POA. Part of the IVOC emissions is not included in conventional inventories, even if it is important for the predicted SOA (Shrivastava et al., 2008; Grieshop et al., 2009; Tsimpidi et al., 2010). Several studies have assumed a 50% addition to the traditional emission inventory (e.g., Shrivastava et al., 2008; Jathar et al., 2011; Tsimpidi et al., 2014) for IVOC emissions but enhancements up to a factor 6.5 have been used in the literature (e.g., Shrivastava et al., 2011). Furthermore, most previous modeling studies typically assumed the same volatility distributions of all emissions independent of their source (e.g. Robinson et al., 2007). However, recent investigations reported significant differences in the volatility distribution of particles emitted from biomass burning, diesel and gasoline vehicle exhausts (May et al., 2013a; May et al., 2013c, b).

The second source of uncertainty is related to the oxidation of the emitted SVOCs and IVOCs. The parameters used by the VBS to simulate this process are the oxidation rate constant, the volatility distribution of the products, and the oxygen mass added per generation of oxidation. The VBS volatility resolution used to represent the SVOC/IVOC volatility range ($3.2\text{x}10^{-1}$ μg m^{-3} < C^* < $3.2\text{x}10^{6}$ μg m^{-3}) affects these parameters as well. A coarse volatility resolution requires a lower effective oxidation rate constant and a more rapid addition of oxygen and reduction in volatility than a finer volatility resolution. A common representation for the oxidation of SVOCs and IVOCs, mainly used by regional models (e.g. Murphy and Pandis, 2009; Tsimpidi et al., 2010; Fountoukis et al., 2011; Tsimpidi et al., 2011; Bergstrom et al., 2012; Athanasopoulou et al., 2013; Fountoukis et al., 2014), is based on the work of Robinson et al. (2007) and Shrivastava et al. (2008) and includes 9 volatility

Atmos. Chem. Phys. Discuss., doi:10.5194/acp-2017-6, 2017
Manuscript under review for journal Atmos. Chem. Phys.
Published: 11 January 2017

Atmospheric Chemistry and Physics Discussions

bins with saturation concentrations ranging from 10^{-2} to 10^{6} μg m^{-3}, an oxidation rate constant of 4×10^{-11} cm^3 $molec^{-1}$ s^{-1} based on Atkinson and Arey (2003), a reduction in volatility by one order of magnitude after each reaction, and a 7.5% net increase in mass to account for the added oxygen. This formulation is rather conservative compared to other studies which have assumed higher reduction in volatility and/or increase in mass. Shrivastava et al. (2011) assumed a 15% increase in mass due to the added oxygen, while Grieshop et al. (2009) and Hodzic et al. (2010) assumed a 40% increase in mass and two orders of magnitude reduction in volatility in each reaction step. Pye and Seinfeld (2010) simulated the POA emissions using two SVOCs (with C^* equal to 20 and 1646 μg m^{-3}) and one IVOC (10^5 μg m^{-3}) and used an oxidation rate constant of 2×10^{-11} cm^3 $molec^{-1}$ s^{-1}, two orders of magnitude reduction in volatility in each reaction, and 50% increase in mass per reaction. Shrivastava et al. (2011) used only two surrogate species (C^* equal to 10^{-2} and 10^5 μg m^{-3}), an oxidation rate constant of 0.57×10^{-11} cm^3 $molec^{-1}$ s^{-1}, seven orders of magnitude reduction in volatility, and 50% increase in mass per reaction. Tsimpidi et al. (2014) used a lower resolution VBS scheme with 4 surrogate species (with C^* 10^{-1}, 10^1, 10^3, and 10^5 μg m^{-3}), an oxidation rate constant of 2×10^{-11} cm^3 $molec^{-1}$ s^{-1}, two orders of magnitude reduction in volatility, and 15% increase in mass per reaction. All of the above schemes should be viewed as parameterizations of the complex reactions that actually take place; the oxidation products can be up to four orders of magnitude lower in volatility than the precursor (Kroll and Seinfeld, 2008). To address this limitation, Jathar et al. (2012) developed a hybrid method to represent the formation of SOA from non-speciated SVOC and IVOC vapors. According to this framework, the first generation of oxidation of SVOC and IVOC is parameterized by fitting to SOA data from smog chamber experiments. Subsequently, the generic multi-generational oxidation scheme of Robinson et al. (2007) was used for the subsequent generation steps.

The third source of uncertainty is related to the scavenging efficiency of gas-phase oxidized SVOCs and IVOCs. The water solubility of these organic vapors is largely unknown and in most OA modeling studies a fixed effective Henry's law constant (e.g., $H = 10^5$ M atm^{-1}) is used for all organic compounds. However, organic vapors become increasingly more hydrophilic during their atmospheric lifetime. Pye and Seinfeld (2010) treated the freshly emitted gas-phase SVOCs as relatively

Atmos. Chem. Phys. Discuss., doi:10.5194/acp-2017-6, 2017
Manuscript under review for journal Atmos. Chem. Phys.
Published: 11 January 2017

Atmospheric Chemistry and Physics Discussions

hydrophobic (H= 9.5 M atm^{-1}) and their oxidation products as moderately hydrophilic (H= 10^5 M atm^{-1}). Hodzic et al. (2014) argued that Henry's law constants have a strong negative correlation with the saturation vapor pressures and depend on the precursor species, the extent of photochemical processing, and the NO_x levels during the formation.

In this work we use ORACLE, a computationally efficient module for the description of OA composition and evolution in the atmosphere (Tsimpidi et al., 2014), to quantify the impact of the main VBS parameters on the model OA predictions. Our main focus is the formation of OA from anthropogenic combustion and open biomass burning sources. We conducted different tests to study the sensitivity of the model predictions to emissions, photochemical aging and scavenging efficiency of LVOCs, SVOCs and IVOCs. The results are compared to the reference simulation and aerosol mass spectrometer (AMS) measurements at multiple locations worldwide following Tsimpidi et al. (2016). Results from these sensitivity tests help identify the major uncertainties of the VBS formulations and give rise to suggestions about potential model improvements.

2 Reference model description and application

2.1 EMAC Model

The ECHAM/MESSy Atmospheric Chemistry (EMAC) model is a numerical chemistry and climate simulation system that includes sub-models describing lower and middle atmosphere processes and their interaction with oceans, land and human influences (Jöckel et al., 2006). EMAC includes submodels that describe gas-phase chemistry (MECCA; Sander et al., 2011), inorganic aerosol microphysics (GMXe; Pringle et al., 2010), cloud microphysics (CLOUD; Jöckel et al., 2006), aerosol optical properties (AEROPT; Lauer et al., 2007), dry deposition and sedimentation (DRYDEP and SEDI; Kerkweg et al., 2006a), cloud scavenging (SCAV; Tost et al., 2006), emissions (ONLEM and OFFLEM; Kerkweg et al., 2006b), and organic aerosol formation and growth (ORACLE; Tsimpidi et al., 2014). The spectral resolution used in this study is T63L31, corresponding to a horizontal grid spacing of 1.875^{o}x1.875^o and 31 vertical layers extending to 25 km altitude. The 11-year period between 2000 and 2010 is simulated, with the first year used as spin-up.

Atmos. Chem. Phys. Discuss., doi:10.5194/acp-2017-6, 2017
Manuscript under review for journal Atmos. Chem. Phys.
Published: 11 January 2017

Atmospheric Chemistry and Physics Discussions

145 **2.2 ORACLE Module**

146 ORACLE is a computationally efficient submodel for the description of organic
147 aerosol composition and evolution in the atmosphere (Tsimpidi et al., 2014). ORACLE
148 simulates a wide variety of semi-volatile organic products separating them into bins of
149 logarithmically spaced effective saturation concentrations. In this study, primary
150 organic emissions from biomass burning and fuel combustion sources are taken into
151 account using separate surrogate species for each source category. These surrogates are
152 subdivided into three groups of organic compounds: LVOCs ($C^*=10^{-2}$ μg m^{-3}), SVOCs
153 ($C^*=10^{0}$ and 10^{2} μg m^{-3}) and IVOCs ($C^*=10^{4}$ and 10^{6} μg m^{-3}). These organic
154 compounds are allowed to partition between the gas and aerosol phases resulting in the
155 formation of POA. Anthropogenic and biogenic VOCs are simulated separately, and
156 their oxidation results in products distributed in four volatility bins with effective
157 saturation concentrations 10^{0}, 10^{1}, 10^{2}, and 10^{3} μg m^{-3}. Gas-phase photochemical
158 reactions that modify the volatility of the organics are taken into account and the
159 oxidation products (SOA-sv, SOA-iv, and SOA-v) of each group of precursors
160 (SVOCs, IVOCs, and VOCs) are simulated separately in the module to keep track of
161 their origin. LVOCs are not allowed to participate in photochemical reactions since
162 they are already in the lowest volatility bin. In total 52 organic compounds are
163 simulated explicitly (26 in each of the gas and aerosol phases). The volatilities of
164 SVOCs and IVOCs are reduced by a factor of 10^{2} as a result of the OH reaction with a
165 rate constant of 2×10^{-11} cm^{3} $molecule^{-1}$ s^{-1} and a 15% increase in mass to account for
166 two added oxygens (Tsimpidi et al., 2014). The model set-up and the different aerosol
167 types and chemical processes that simulated by ORACLE in this study are illustrated
168 in Figure 1a. More details about ORACLE can be found in Tsimpidi et al. (2014).
169

170 **2.3 Emission inventory**

171 The CMIP5 RCP4.5 emission inventory (Clarke et al., 2007) is used for the
172 anthropogenic primary organic aerosol emissions from fuel combustion and biomass
173 burning. The open biomass burning emissions from savanna and forest fires are based
174 on the Global Fire Emissions Database (GFED v3.1; van der Werf et al., 2010). In
175 order to convert the emitted organic carbon (OC) to organic mass (OM), OM/OC
176 factors of 1.3 and 1.6 have been used for the anthropogenic and biomass burning
177 emissions, respectively (Aiken et al., 2008; Canagaratna et al., 2015). Furthermore,

Atmos. Chem. Phys. Discuss., doi:10.5194/acp-2017-6, 2017
Manuscript under review for journal Atmos. Chem. Phys.
Published: 11 January 2017

Atmospheric Chemistry and Physics Discussions

emission fractions are used to distribute the OM to the volatility bins used by ORACLE. The sum of the emission fractions used for the volatility bins with C* ≤ 10^4 is unity since current emission inventories are based on samples collected at aerosol concentrations up to 10^4 μg m^{-3} (Shrivastava et al., 2008; Robinson et al., 2010). Additional emission fractions can be assigned to the volatility bins with C* > 10^4 based on dilution experiments (Robinson et al., 2007).

In this study we assume that anthropogenic fuel (fossil and biofuel) combustion emissions cover a range of volatilities from 10^{-2} to 10^6 μg m^{-3} and the additional IVOC emissions are 1.5 times the traditional POA emissions (Robinson et al., 2007); therefore, the sum of the emission fractions for the fuel combustion emissions is 2.5 (Figure 2a). Biomass burning emissions are assumed to cover a range of volatilities from 10^{-2} to 10^4 (May et al., 2013a), therefore, no IVOC emissions are assumed from biomass burning sources and the sum of their emission factors is unity (Figure 2a). Overall, the decadal average global emission flux of primary organic emissions is 44 Tg yr^{-1} from anthropogenic combustion sources and 28 Tg yr^{-1} from open biomass burning sources.

3 Sensitivity Simulations

All sensitivity calculations are conducted for the same 11-year period as the reference simulation, the results of which have been analyzed by (Tsimpidi et al., 2016). Table 1 summarizes the general characteristics of the sensitivity simulations. A detailed description is provided below.

3.1 Sensitivities to emissions

The emissions of LVOCs, SVOCs and IVOCs are a key input for the accurate description of atmospheric OA. To quantify the sensitivity of the reference case results to the LVOC, SVOC and IVOC emissions, three simulation tests have been designed. Figure 2 summarizes the emission factors used for the volatility distribution of the emissions and the emission rate of each volatility bin for the reference and the sensitivity tests. More specifically:

Low volatility: In this sensitivity simulation, we assume zero emissions of IVOCs to quantify their contribution to the formation of global SOA. Therefore, the fuel

Atmos. Chem. Phys. Discuss., doi:10.5194/acp-2017-6, 2017
Manuscript under review for journal Atmos. Chem. Phys.
Published: 11 January 2017

combustion and biomass burning emissions are distributed only in the LVOCs (10^{-2} μg m^{-3}) and SVOCs (10^{0} and 10^{2} μg m^{-3}) volatility bins and the sum of their emission fractions is equal to unity (Figure 2b). The decadal average global emission flux of primary organic emissions in this test is 18 Tg yr^{-1} from anthropogenic combustion sources and 28 Tg yr^{-1} from open biomass burning sources (Table 1).

High IVOCs: To estimate an upper limit of the IVOC contribution to the formation of SOA, a sensitivity simulation is conducted where the emissions of IVOCs are increased by an additional factor of 1.5 times the POA emissions distributed in the volatility bins with C^* of 10^{4} and 10^{6} μg m^{-3} (Figure 2c). The LVOC and SVOC emissions are the same as in the reference simulation. Overall, the decadal average global emission flux of primary organic emissions in this sensitivity test is 71 Tg yr^{-1} for both anthropogenic and open biomass burning sources (Table 1).

Alternative POA emissions: To investigate the sensitivity of the model results to the magnitude of the POA emissions, we have utilized the AEROCOM database for the POA emissions from anthropogenic combustion sources (Dentener et al., 2006) and the CMIP5 RCP4.5 emission inventory for the POA emissions from open biomass burning sources. These emission inventories include 36% lower POA emissions from anthropogenic combustion sources and 33% higher POA emissions from open biomass burning sources on average over the decade 2000-2010 compared to the reference simulation. The assumed volatility distributions are the same as in the reference simulation. The decadal average global emission flux of primary organic emissions in this case is 29 Tg yr^{-1} from anthropogenic combustion sources and 38 Tg yr^{-1} from open biomass burning sources (Table 1).

3.2 Sensitivity to chemistry

The photooxidation of SVOCs and IVOCs emitted from fuel combustion and biomass-burning sources can lead to the formation of substantial SOA mass on a global scale (Jathar et al., 2011; Tsimpidi et al., 2014). To evaluate the sensitivity of the model to the parameters used to describe the aging process we have conducted three sensitivity simulations described below.

Atmos. Chem. Phys. Discuss., doi:10.5194/acp-2017-6, 2017
Manuscript under review for journal Atmos. Chem. Phys.
Published: 11 January 2017

Atmospheric Chemistry and Physics Discussions

High reaction rate constant: In this simulation we investigate the sensitivity of the results to the rate constant used for the gas-phase photooxidation of SVOCs and IVOCs with OH. We assume that the corresponding oxidation rate constant is twice that of the reference simulation and equal to $4x10^{-11}$ cm^3 $molecules^{-1}$ s^{-1}. All other parameters remained the same as in the reference simulation (Table 1).

Alternative aging scheme: To quantify the sensitivity of the results to the aging scheme, we designed a sensitivity case in which the aging scheme of Robinson et al. (2007) is used (Figure 1b). Based on this implementation, we are using nine volatility bins (compared to 5 in the reference simulation) to distribute the primary emissions into LVOCs (10^{-2} and 10^{-1} μg m^{-3}), SVOCs (10^0, 10^1, and 10^2 μg m^{-3}), and IVOCs (10^3, 10^4, 10^5, and 10^6 μg m^{-3}). This model set up is based on the formulation proposed by (Shrivastava et al., 2008). The volatility distribution of anthropogenic combustion and open biomass burning emissions is shown in Figure 2d. The sum of these emission factors is the same as in the reference simulation (2.5 for fuel combustion and 1 for biomass burning). However, the relative importance of SVOC and IVOC to total OA emissions is changed compared to the reference simulation. In the sensitivity simulation the fraction of SVOCs to the total emissions is 20% for fOA and 60% for bbOA (Figure 2d), compared to 32% and 70%, respectively, in the reference simulation (Figure 2a). Furthermore, the saturation concentration of the organic vapors reacting with OH is reduced by a factor of 10 (instead of 100 in the reference simulation) with a rate constant of $4x10^{-11}$ cm^3 $molec^{-1}$ (double the value used in the reference simulation) and a 7.5% increase in mass to account for one added oxygen (half the value used in the reference simulation). The formation of SOA from LVOCs is possible in this configuration (contrary to the reference simulation) due to the presence of two species in the LVOC volatility range ($C^* < 3.2x10^{-1}$ μg m^{-3}). Overall, in this simulation, 46 surrogate organic aerosol species are used to track the source- and volatility-resolved OA components compared to 26 aerosol species in the reference simulation.

Hybrid aging scheme: The reference and alternative aging scheme simulations assume that the volatility of the organic vapor precursors is reduced by two and one orders of magnitude, respectively, after each oxidation step. However, photooxidation

Atmos. Chem. Phys. Discuss., doi:10.5194/acp-2017-6, 2017
Manuscript under review for journal Atmos. Chem. Phys.
Published: 11 January 2017

Atmospheric Chemistry and Physics Discussions

reactions of IVOCs can create products with a volatility 1 to 4 orders of magnitude lower (Kroll and Seinfeld, 2008). Furthermore, recent experiments indicate that the reduction in volatility due to oxidation reactions changes as the organic molecules become more oxygenated and fragmentation becomes important (Chacon-Madrid et al., 2013). To investigate the effect of these assumptions on the predicted global SOA burden, we have modified the OA chemistry mechanism to include a hybrid method to calculate the SOA formation from the oxidation of IVOCs based on the approach of (Jathar et al., 2012). The SVOC oxidation scheme remains the same as in the reference. The hybrid scheme distributes the IVOC first generation oxidation products over a range of volatilities, with larger reductions in volatility compared to the reference simulation. The oxidation of each IVOC is assumed to result in the formation of two condensable organic gases with four and six orders of magnitude lower volatility and aerosol yields equal to 0.71 and 0.115, respectively (Jathar et al., 2014) (Figure 1c). Then, the reference oxidation scheme is used for subsequent oxidation of these products assuming a factor of 100 reduction in volatility with 15% increase in mass. The photo-oxidation of SVOCs and IVOCs in the hybrid aging scheme is described by the following reactions:

$$SVOC_i + OH \rightarrow 1.15\ SOG\text{-}sv_{i-1} \quad (R1)$$

$$SOG\text{-}sv_i + OH \rightarrow 1.15\ SOG\text{-}sv_{i-1} \quad (R2)$$

$$SOG\text{-}sv_i \leftrightarrow SOA\text{-}sv_i \quad (R3)$$

$$IVOC_i + OH \rightarrow 0.71\ SOG\text{-}iv_{i-2} + 0.115\ SOG\text{-}iv_{i-3} \quad (R4)$$

$$SOG\text{-}iv_i + OH \rightarrow 1.15\ SOG\text{-}iv_{i-1} \quad (R5)$$

$$SOG\text{-}iv_i \leftrightarrow SOA\text{-}iv_i \quad (R6)$$

This representation is more consistent with SOA formation from VOCs and provides in principle at least a more realistic representation of SOA formation from IVOCs.

3.3 Sensitivities to scavenging

The wet and dry removal the organic vapours from the atmosphere depends on their ability to partition into water which is commonly expressed by their Henry's law

Atmos. Chem. Phys. Discuss., doi:10.5194/acp-2017-6, 2017
Manuscript under review for journal Atmos. Chem. Phys.
Published: 11 January 2017

Atmospheric Chemistry and Physics Discussions

constant (H). Two sensitivity simulations where performed to investigate the effect of this uncertain parameter.

Low solubility: To test the sensitivity of the results to the solubility of the SVOC and IVOC vapors, we have conducted a simulation using a Henry's law constant two orders of magnitude lower than the reference and equal to 10^3 M atm^{-1} for both primary and secondary SVOCs/IVOCs.

Variable solubility: The photochemical aging of organic vapors results on average in less volatile and more hydrophilic products (Jimenez et al., 2009). To quantify the effect of this change on the model results we have conducted a sensitivity simulation in which the fresh SVOCs and IVOCs are hydrophobic with H =10 M atm^{-1} and become more hydrophilic after their photochemical oxidation with an H =10^5 M atm^{-1}.

4 Reference simulation results and evaluation

The predicted decadal average surface concentrations of total OA, POA, SOA-sv, and SOA-iv for the reference simulation are shown in Figure 3. High POA concentrations are predicted over regions affected by biomass burning (i.e., the tropical and boreal forests) as well as over the industrialized regions of the Northern Hemisphere where strong fossil and biofuel combustion sources are located (i.e., Eastern and Southern Asia, Central and Eastern Europe, Western and Eastern US). Further downwind of the sources, the POA concentration decreases substantially due to dilution and evaporation (Figure 3b). On the other hand, the predicted SOA-sv and SOA-iv concentrations are high over a wide area downwind of the polluted urban areas and the major rainforests (Figure 3c and 3dc) due to the transport of IVOCs and SVOCs and their continued chemical transformations. Since IVOC emissions from anthropogenic sources are assumed to be two times higher than SVOC emissions (Figure 1a), predicted SOA-iv is higher than SOA-sv over populated areas (Figure 3c and 3d). On the other hand, over the tropical rainforests, SOA-sv and SOA-iv concentrations are similar due to the low fraction of IVOCs assumed for the open biomass burning OA emissions. Overall, the reference simulation yields a tropospheric OA burden of 1.98 Tg consisting of 12% POA, 18% SOA-sv, 32% SOA-

Atmos. Chem. Phys. Discuss., doi:10.5194/acp-2017-6, 2017
Manuscript under review for journal Atmos. Chem. Phys.
Published: 11 January 2017

Atmospheric Chemistry and Physics Discussions

iv, and 38% SOA-v. More details about the reference case results can be found in Tsimpidi et al. (2016).

A comprehensive AMS dataset from field campaigns performed in the Northern Hemisphere during 2001-2010 (Tsimpidi et al., 2016) has been used to evaluate the model performance for each simulation. The mean bias (MB), mean absolute gross error (MAGE), normalized mean bias (NMB), normalized mean error (NME), and the root mean square error (RMSE) are used to assess the model performance for POA (versus AMS hydrocarbon-like aerosol (HOA); Table 2) and SOA (versus AMS oxygenated organic aerosol (OOA); Table 3). Tsimpidi et al. (2016) have shown that, as expected the model underestimates the concentrations of POA and SOA over urban locations due to its coarse resolution and missing sources in the emission database (e.g., cold vehicle start and wood burning emissions in winter). Therefore, urban locations are excluded from our analysis in order to avoid misinterpretation of the sensitivity results and their effects on OA model performance. A comprehensive analysis of the model evaluation based on the reference scenario results can be found in Tsimpidi et al. (2016) and will be used here as a reference for analysing the effect of each sensitivity scenario on the performance of the model. EMAC reproduces POA levels with very little bias (NMB= -3%; Table 2). On the other hand, OOA concentrations are underpredicted (-31%; Table 3) indicating that the model may be missing an important source or formation pathway of SOA especially in winter (Tsimpidi et al., 2016) or may be removing the corresponding pollutants faster.

5 Sensitivity to emission factors

5.1 Low volatility

In the first sensitivity test, the IVOC emissions are set to zero and only semi-volatile organic compounds are emitted. This is accompanied by an increase of SVOC emissions from anthropogenic and open biomass burning sources by 100% and 40%, respectively. This initial partitioning of the emissions favors the particulate phase, resulting in an increase of POA compared to the reference scenario (Figure 4a). The largest fPOA and bbPOA increases are predicted over Eastern China (4.3 μg m^{-3}) and the Congo Basin (3.9 μg m^{-3}), respectively. The higher SVOC emissions in the sensitivity simulation result in an increase of the simulated SOA-sv concentrations as well (Figure 5a). However, since a large fraction of the emitted SVOCs remains in the

Atmos. Chem. Phys. Discuss., doi:10.5194/acp-2017-6, 2017
Manuscript under review for journal Atmos. Chem. Phys.
Published: 11 January 2017

particle phase, the SOA-sv concentration increase is smaller than the corresponding changes in POA. Relatively strong fSOA-sv and bbSOA-sv increases are found over the Indo-Gangetic Plane (IGP) (0.4 μg m^{-3}) and the Congo Basin (1.3 μg m^{-3}), respectively. The "low volatility" simulation does not predict any SOA-iv as it assumes zero IVOC emissions. Therefore, SOA-iv concentrations are zero around the globe, resulting in substantial decreases in areas where the reference simulation predicts high SOA-iv levels (Figures 3dc and 6a).

The significant decrease of organic emissions from anthropogenic sources (Table 1) due to the lack of IVOC emissions results in an overall decrease of total OA concentrations by up to 5 μg m^{-3} over anthropogenically polluted regions (Figure 7a). On the other hand, organic emissions from open biomass burning sources remain at the same level as the reference simulation (Table 1), however, they are assumed to have lower volatility. This results in an increase of total OA concentrations in the sensitivity simulation by up to 2 μg m^{-3} over the tropical and boreal forests. Overall, the calculated tropospheric burden of POA in the sensitivity simulation increases by around 50% due to the increase of the SVOC emissions (Table 2). For the same reason, the tropospheric fSOA-sv and bbSOA-sv burdens increase by 14% and 39%, respectively. Nevertheless, the absence of IVOC emissions, and thus the significant decrease of anthropogenic organic compound emissions, results in a decrease of the total OA tropospheric burden by 23%. This result emphasizes the importance of the volatility distributions used in the simulation and the contribution of IVOC emissions to SOA formation on a global scale.

The simulated POA in the reference model configuration is very close to the average HOA concentrations derived from the AMS measurements (Table 3). Therefore, assuming lower volatility of the organic emissions results in overprediction (NMB=43%). However, the performance of the model is significantly improved during winter (Figure 8) since POA concentrations during that season were underpredicted (NMB=-37%; Tsimpidi et al., 2016). On the other hand, during spring the overestimate of POA increases in the sensitivity simulation (NMB=86%) compared to the reference (NMB=26%). For summer and autumn, the performance of the model changes from a slight underestimation of POA in the reference (NMB=-15%) to a slight overprediction in the sensitivity test (NMB=30%). The performance of the model in reproducing the OOA concentrations worsens in this sensitivity

Atmos. Chem. Phys. Discuss., doi:10.5194/acp-2017-6, 2017
Manuscript under review for journal Atmos. Chem. Phys.
Published: 11 January 2017

simulation (Table 4). OOA was underpredicted by the model reference simulation (NMB=-31%), therefore, by neglecting SOA formation from IVOC emissions in the sensitivity run results in an even larger OOA underestimation (NMB=-52%). The performance of the model does not change significantly during winter (Figure 8) since the simulated SOA formation during this season is low (Tsimpidi et al., 2016). The highest change in model performance occurs during spring when SOA is predicted to reach the annual maximum (Tsimpidi et al., 2016); the predicted underestimation of OOA increases from 20% in the reference to 50% in the sensitivity simulation. These results indicate that the omission of IVOCs as a source of SOA in atmospheric models can result in a significant underestimation of OA concentrations, especially during periods where formation of SOA is strong.

5.2 High IVOCs

In the second sensitivity simulation, the increased IVOC emissions result in an increase of total organics by 60%, and 150% from anthropogenic and open biomass burning sources, respectively (Table 1). These additional organic emissions are distributed only in the intermediate volatility bins, therefore, their impact on the simulated POA and SOA-sv levels is marginal (Figures 4b and 5b, respectively). POA increases, up to 0.6 μg m^{-3} over Eastern China, while SOA-sv decreases, up to 0.3 μg m^{-3} over the Congo Basin. This effect can be explained by the assumption that SOA-sv and SOA-iv form a pseudo-ideal solution. As a result, the increased SOA-iv concentrations calculated in the sensitivity simulation favor the partitioning of the fresh SVOCs into the aerosol phase, forming additional POA. At the same time, SVOCs decrease in the gas-phase and therefore the formation of SOA-sv is reduced in the sensitivity simulation. As expected, the largest effect is found for SOA-iv (Figure 6b). The significant increase of IVOC emissions results in large changes of SOA-iv over areas close to anthropogenic sources (up to 5.7 μg m^{-3} over the IGP) and biomass burning regions (up to 5.3 μg m^{-3} over the Congo Basin). The increase of SOA-iv dominates the effect on total OA concentrations that increase up to 6 μg m^{-3} (Figure 7b). Overall, the predicted changes of the tropospheric burden of POA and SOA-sv are small (Table 2). However, the tropospheric burdens of fSOA-iv and bbSOA-iv increase by 88% and 115%, respectively, resulting in an increase of the total OA burden by 38%.

Atmos. Chem. Phys. Discuss., doi:10.5194/acp-2017-6, 2017
Manuscript under review for journal Atmos. Chem. Phys.
Published: 11 January 2017

Atmospheric Chemistry and Physics Discussions

441 The additional IVOC emissions assumed in this sensitivity test do not affect the
442 performance of the model for POA. On the other hand, these additional emissions
443 bring the predicted SOA concentrations closer to the measured OOA levels (Table 4;
444 Figure 8). The NMB improves from -31% in the reference simulation to -10%. With
445 the exception of winter, where the model still underpredicts OOA levels (MB=2.2 μg
446 m^{-3}, Figure 8), the performance of the model for SOA improves with seasonal NMB
447 ranging from -16% (during summer) to 11% (during spring); compared to -33% and
448 -20% for the reference model, respectively. The improved performance of the model
449 due to the increase of IVOC emissions supports the hypothesis that the IVOC
450 emissions may have been underestimated in previous modeling studies that assumed
451 IVOC/POA =1.5 (Ots et al., 2016).
452
453 **5.3 Alternative POA emissions**
454 The final emission sensitivity test is used to estimate the uncertainty introduced by
455 the choice of emission database. The inventories used in the sensitivity simulation
456 assume 36% lower fuel combustion OA emissions and 33% higher biomass burning
457 OA emissions compared to the reference simulation, while the total OA emissions are
458 only reduced by 9%. Since the volatility distribution of the emissions is identical to
459 the reference simulation, the fractional changes of the calculated POA, SOA-sv, SOA-
460 iv are also similar (Table 4). The tropospheric burden of fOA (the sum of fPOA,
461 fSOA-sv, and fSOA-iv) decreases by 34%. On the other hand, bbOA (the sum of
462 bbPOA, bbSOA-sv, and bbSOA-iv) increases by 11%. Overall, the total tropospheric
463 OA burden increases by only 4%. The changes in fOA and bbOA concentrations,
464 however, are not spatially uniform. Over Europe, fOA decreases everywhere, up to
465 3.3 μg m^{-3}, except in Paris where fOA increases by 0.24 μg m^{-3}. Over the US fOA
466 slightly increases (mostly over the northeast by up to 0.6 μg m^{-3}), while it decreases
467 over Mexico by as much as 1.7 μg m^{-3}. The largest fOA change is predicted over Asia
468 where fOA decreases significantly, up to 8.3 μg m^{-3}, mostly over East Asia and the
469 IGP. bbOA decreases over the boreal forests (up to 3.6 μg m^{-3}), while it increases
470 significantly over the Southeast Asian tropical forests by up to 14 μg m^{-3}. Over the
471 Amazon and Congo forests, bbOA concentrations change significantly (the bbOA
472 changes vary from -2.4 to 3.3 μg m^{-3} in the Amazon, and from -5.3 to 7.8 μg m^{-3} in
473 Congo) but the average bbOA concentration over both regions remains the same.

Atmos. Chem. Phys. Discuss., doi:10.5194/acp-2017-6, 2017
Manuscript under review for journal Atmos. Chem. Phys.
Published: 11 January 2017

Atmospheric Chemistry and Physics Discussions

Overall, the fOA and bbOA emission changes lead to total OA increases over the tropical and boreal forests and decreases over anthropogenic areas (Figure 7c).

The lower OA emissions used in the sensitivity simulation (especially over China and Europe) result in a reduction of both total POA and SOA concentrations (Tables 2 and 3). Consequently, the model now underestimates POA with NMB=-25% and SOA with NMB=-40%. These results suggest that the use of the CMIP5 RCP4.5 emission inventory in EMAC results in OA concentrations that agree more closely to the measurements compared to the AEROCOM database. It also underscores the large uncertainty associated with primary OA emissions.

6 Sensitivity to aging reactions

6.1 Higher aging reaction rate

In this sensitivity simulation, the photochemical reaction rate constant for SVOCs and IVOCs has been doubled compared to the reference. This results in an increase of SOA-sv and SOA-iv concentrations worldwide (Figures 5d and 6d). SOA-sv increases, up to 0.65 μg m^{-3}, mostly over the tropics and the polluted regions of Eastern China and the IGP (Figure 5d). The effect on SOA-iv concentrations is even more significant since IVOCs undergo more oxidation steps before forming SOA than SVOCs. SOA-iv increased by up to 2.4 μg m^{-3} mostly over the IGP and Eastern China (Figure 6d). The SOA-iv increase over the tropics is smaller (up to 0.8 μg m^{-3}) due to the assumed low fraction of IVOCs in biomass burning emissions. Overall, the tropospheric burdens of SOA-sv and SOA-iv both increase by 0.04 Tg (or 11% and 7%, respectively). POA is not expected to be affected directly by the change of the reaction rate constant. However, the substantial reduction of gas-phase SVOCs (due to their increased reactivity) results in the re-evaporation of POA to achieve equilibrium, reducing its concentration (Figure 4d) mainly over the tropics (up to 0.21 μg m^{-3}). This results in an overall decrease of the tropospheric POA burden by 8%. Following the significant increase of both SOA-sv and SOA-iv, total OA increases worldwide by up to 3 μg m^{-3} (Figure 7d). Overall, the tropospheric burden of total OA increases by 4%.

The model performance for POA is not affected by the change of the reaction rate constant (Table 2) since POA remains largely unchanged over the Northern Hemisphere (Figure 4d). On the other hand, the performance of the model regarding

Atmos. Chem. Phys. Discuss., doi:10.5194/acp-2017-6, 2017
Manuscript under review for journal Atmos. Chem. Phys.
Published: 11 January 2017

SOA is significantly improved (Table 3). The underestimation of SOA by the model is reduced (NMB=-22%) compared to the reference (NMB=-31%). The best performance is found during spring (NMB=-7%) when the calculated SOA is almost unbiased. However, during winter, the model still severely underestimates SOA (NMB=-77%), which indicates that the gas-phase oxidation of SVOCs and IVOCs does not suffice to explain the underprediction of SOA in winter.

6.2 Alternative aging scheme

In this sensitivity simulation we used the chemical aging scheme of Robinson et al. (2007) which is currently the most commonly used in VBS models. This aging scheme is accompanied by changes in the number of volatility bins used and the assigned emission factors, the oxidation rate constant, the volatility reductions after each oxidation step, and the increase in mass due to added oxygen (as discussed in Sect. 3.2). The changes in the number of volatility bins and the emission factors used for the SVOCs (Figure 2d) result in reduced condensation of SVOCs into the particulate phase during the initial partitioning and therefore to a significant decrease of POA (Figure 4e). The decrease of POA is global and most prominent over Eastern China (up to 9.3 μg m^{-3}). This reflects a significant change in the tropospheric burdens of both fPOA and bbPOA by 65% and 38%, respectively.

Furthermore, the reduced fraction of SVOCs to total OA emissions (see Section 3.2) results in a worldwide decrease of SOA-sv (Figure 5e) and an increase of SOA-iv (Figure 6e). SOA-sv decreases up to 1.8 μg m^{-3} over the Congo Basin and the IGP. Similar to POA, the tropospheric burden of fSOA-sv and bbSOA-sv decreases by 68% and 47%, respectively. On the other hand, the increase in SOA-iv, due to the increase in the IVOC fraction of the emissions, is not as strong as the decrease of SOA-sv (Table 4). This is due to the slower aging in the sensitivity simulation (Figure 1b), compared to the reference (Figure 1a), which limits the formation of SOA from IVOCs. SOA-iv increases up to 0.9 μg m^{-3} over the Congo Basin and the IGP, while it locally decreases by 0.1 μg m^{-3} over Beijing, for example. The tropospheric burden of fSOA-iv and bbSOA-iv increases by 14% and 30%, respectively. Overall, the sum of SOA-sv and SOA-iv decreases by 7% due to the slower aging in this sensitivity simulation. Following the simultaneous decrease of both POA and SOA, total OA

Atmos. Chem. Phys. Discuss., doi:10.5194/acp-2017-6, 2017
Manuscript under review for journal Atmos. Chem. Phys.
Published: 11 January 2017

decreases worldwide by up to 11 μg m^{-3} (Figure 7e) and its tropospheric burden is reduced by 0.2 Tg (or 10%).

The reduction of both modelled POA and SOA results in reduced agreement of the model with AMS measurements. Especially for POA, the modeled concentrations decrease by 67% in the sensitivity simulation, resulting in a significant underprediction of AMS-HOA (NMB=-67%). Modelled SOA also decreases (by 10%) in the sensitivity simulation, which degrades the model agreement with AMS-OOA measurements (NMB=-38%). This sensitivity test underscores the significance of the volatility distribution of the organic emissions and the associated aging scheme.

6.3 Hybrid aging scheme

The final chemistry sensitivity simulation focuses on the photochemical aging of IVOCs and assumptions regarding the first oxidation step. The approach used here is similar to the oxidation of the traditional VOCs, in contrast with the reference where the oxidation of IVOCs produces only one product with two orders of magnitude reduced volatility. However, the stoichiometric coefficient used in the reference (equal to 1.15) is higher than the aerosol yields used in the sensitivity simulation (Section 3.2). This results in a reduction of SOA-iv concentrations by up to 2.2 μg m^{-3} (Figure 6f). Since the chemical scheme for SVOCs is identical in both the reference and the sensitivity simulations, no significant change is found in either SOA-sv or POA (Figure 5f and 4f, respectively). The decrease of SOA-iv concentrations has a marginal effect on the initial partitioning of SVOC emissions resulting in slightly less POA and more SOA-sv (by up to 0.1 μg m^{-3} in either case). Therefore, total OA concentrations are reduced worldwide following the decrease of SOA-iv. Overall, the tropospheric burden of SOA-iv decreases by 37% in the sensitivity simulation resulting in a decrease of total OA by 13% (Table 4).

The simulated POA concentrations remain almost unchanged in the sensitivity simulation; therefore, similar to the reference, the calculated POA is unbiased compared to measurements (Table 2). On the other hand, the lower SOA-iv concentrations calculated by the model in this sensitivity test aggravate the underestimation of OOA by the model (NMB=-39%). The decrease of modelled SOA-iv concentrations is larger during spring (13%) and the calculated NMB for SOA deteriorates from -20% in the reference to -30% in the sensitivity simulation.

Atmos. Chem. Phys. Discuss., doi:10.5194/acp-2017-6, 2017
Manuscript under review for journal Atmos. Chem. Phys.
Published: 11 January 2017

Atmospheric Chemistry and Physics Discussions

572

573 **7 Sensitivity to wet/dry removal of organic vapors**

574 **7.1 Reduced Henry's law constant**

575 In this sensitivity test we used a Henry's law constant that is two orders of
576 magnitude lower than in the reference simulation (see Section 3.3) for the gas-phase
577 SVOCs and IVOCs. This change decreases their removal rate, thus increasing their
578 lifetime and the concentrations of both POA (due to the condensation of the fresh
579 SVOCs) and SOA (due to the condensation of the chemically aged SVOCs and
580 IVOCs). POA increases up to 0.7 μg m^{-3} over Eastern China (Figure 4g) where POA
581 concentrations are relatively high (Figure 3b), however, the increase of POA in the
582 rest of the world is less than 0.2 μg m^{-3} (Figure 4g). SOA-sv increases up to 0.2 μg
583 m^{-3} mostly over the Congo Basin and the IGP (Figure 5g). The most significant
584 change is calculated for SOA-iv. SOA-iv is formed from gases (i.e., IVOCs) that need
585 to go through more than two oxidation steps to be able to condense to the aerosol
586 phase (in comparison to only one oxidation step for SVOCs). Therefore, by lowering
587 the Henry's law constant of IVOCs we prolong the lifetime of SOA-iv precursors, and
588 their ability to undergo multiple oxidation steps and produce aerosols. This results in a
589 significant increase of SOA-iv by up to 1.2 μg m^{-3} (Figure 6g). Total OA increases by
590 up to 2 μg m^{-3} due to the simultaneous increase of both POA and SOA (Figure 7g).
591 Overall, the tropospheric burden of SOA-iv increases by 17% and of total OA by 8%.
592 It is also worth noticing that the tropospheric burden of fOA (sum of fPOA, fSOA-sv,
593 and fSOA-iv) increases by 18% compared to an increase of 5% of the bbOA (sum of
594 bbPOA, bbSOA-sv, and bbSOA-iv). The above results emphasize the significance of
595 the removal of organic vapors for the calculated OA concentrations, and corroborate
596 the importance of constraining the Henry' law constants of SVOCs and more
597 importantly of IVOCs.

598 The change of Henry's law constant of SVOCs does not affect the model
599 performance for POA significantly. POA slightly increases (by 4%), eliminating the
600 already low model bias (Table 2). The SOA increase (by 12%) in the sensitivity
601 simulation (mainly due to the increased SOA-iv) results in reduced SOA
602 underestimation (Table 2). In both POA and SOA cases the effect is more important
603 during winter, when wet removal is most efficient, and lower during summer. POA
604 increases during winter by 10% while during summer it remains unchanged. SOA

Atmos. Chem. Phys. Discuss., doi:10.5194/acp-2017-6, 2017
Manuscript under review for journal Atmos. Chem. Phys.
Published: 11 January 2017

605 increases during winter by 26% and during summer by only 3%, with spring and
606 autumn in between (~12%). Despite the wintertime POA and SOA increase in this
607 sensitivity simulation, the model still underestimates POA (NMB=-31%) and SOA
608 (NMB=-78%) during this season (Figure 8).
609
610 **7.2 Different Henry's law constant for POA and SOA**
611 In the last sensitivity test we assume that the freshly emitted SVOCs and IVOCs
612 are hydrophobic (with the Henry's law constant *H* being 4 orders of magnitude lower
613 than the reference) while after photochemical aging *H* increases to match the value
614 used in the reference (see Section 3.3). POA increases up to 0.7 μg m^{-3}, mostly over
615 Eastern China and to a lesser degree over Eastern Europe and Russia (Figure 4h).
616 SOA-sv increases up to 0.2 μg m^{-3}, mostly over the tropical forests of Central Africa
617 and Southeastern Asia, as well as over Eastern China and the IGP (Figure 5h). SOA-
618 iv also increases by up to 1 μg m^{-3} (Figure 6h) because fresh IVOCs are more
619 hydrophobic in the sensitivity simulation, therefore, the time available to react with
620 OH is extended, forming additional SOA-iv. Total OA concentrations increase by up
621 to 2 μg m^{-3} over Eastern China (Figure 7h). The tropospheric burden of total OA
622 increases by 8% in this sensitivity test with the strongest increase coming from fSOA-
623 iv (21%).
624 Both the predicted POA and SOA increase in the sensitivity simulation by 6% and
625 12% respectively. This results in a small overprediction of POA (NMB=4%),
626 compared to a small underprediction in the reference (NMB=-3%). For SOA, NMB
627 improves in the sensitivity simulation (NMB=-23%) compared to the reference (-
628 31%). Similar to the previous sensitivity test (Section 7.1) the effect is more relevant
629 during winter (POA and SOA increase by 9% and 36%, respectively), followed by
630 spring (POA and SOA increase by 8% and 16%, respectively) and autumn (POA and
631 SOA increase by 7% and 10%, respectively), and is small during summer (POA and
632 SOA increase by 2% and 5%, respectively) (Figures 8). This results in an improved
633 model performance for both POA and SOA during all seasons. The highest
634 improvement is found for SOA during spring when the NMB is reduced to -6% from
635 -20% in the reference. Despite the significant increase of SOA concentrations during
636 winter (by 36%), the model still strongly underestimates SOA (NMB=-76%),
637 indicating that the model underperprediction of OOA cannot be attributed solely to

Atmos. Chem. Phys. Discuss., doi:10.5194/acp-2017-6, 2017
Manuscript under review for journal Atmos. Chem. Phys.
Published: 11 January 2017

errors in the simulation of removal processes. Therefore, we expect that the discrepancy in this season is related to sources that are missing or underestimated in emission inventories, such as residential wood combustion in winter (Denier van der Gon et al., 2015) and additional oxidation pathways.

8 Summary and conclusions

We investigated the effect of parameters and assumptions that control the emissions, photochemical aging, and scavenging efficiency of LVOCs, SVOCs and IVOCs on the simulated OA concentrations. We used the organic aerosol module ORACLE, based on the VBS framework, in the EMAC global chemistry-climate model. A global dataset of AMS measurements has been used to evaluate the predicted POA and SOA concentrations, based on a number of sensitivity tests.

The results show that total OA concentrations are sensitive to the emissions of IVOCs. By neglecting these emissions, the model produces unrealistically low SOA concentrations resulting in the poorest model performance (NMB=-52%) compared to the other eight simulations conducted (Table 3). Conversely, increasing the IVOC emissions substantially improved the SOA model results, leading to the best model performance (NMB=-10%). These results emphasize the need to accurately estimate the IVOC emissions independently. The use of a more accurate POA emission inventory is found to be of prime importance for the model performance, especially to improve simulated POA concentrations in winter. In our tests, using an alternative POA emission inventory led to a NMB of -25% compared to a low bias in the performance of the reference model.

Sensitivity tests of the photochemical aging of SVOCs and IVOCs indicate the importance of the OH-reaction rate. Assuming an increased reactivity of SVOC and IVOC with OH improves the model results for SOA (NMB=-22%). This is even more important for the IVOCs, which participate in a larger number of photochemical reactions during atmospheric transport compared to the SVOCs. Another assumption tested is that oxidation reactions of IVOCs are similar to many other VOCs, and produce partly oxidized compounds with several orders of magnitude lower volatilities. Despite the strong volatility reduction of the IVOC oxidation products, the performance of the model was similar to the reference simulation since the IVOC aerosol yields were lower compared to the stoichiometric coefficient used in the

Atmos. Chem. Phys. Discuss., doi:10.5194/acp-2017-6, 2017
Manuscript under review for journal Atmos. Chem. Phys.
Published: 11 January 2017

reference. The use of an alternative aging scheme (based on Robinson et al., 2007) resulted in lower SOA concentrations since the photochemical aging of SVOCs and IVOCs was less effective. This led to a slight reduction in model performance for SOA (Table 3). In this sensitivity test the fraction of SVOCs to total OA emissions was lower compared to the reference, resulting in a significant reduction of POA and a reduced model performance (NMB=-67%). This underscores the significance of the assumed volatility distribution of OA emissions.

The calculated OA concentrations are highly sensitive to the scavenging efficiency of the gas-phase SVOCs and IVOCs, expressed by the Henry's law constant (*H*). Reducing *H* resulted in an increase of both POA and SOA concentrations, especially from the oxidation of IVOCs. This increase yielded improved model performance, particularly for SOA (Table 3). Assuming different hygroscopicity for the freshly emitted and the photochemically processed SVOCs and IVOCs resulted in similar improvement of the model results (Tables 2 and 3). In this sensitivity test, the simulated POA improved substantially during winter (NMB=-29%) during which the model has difficulties reproducing AMS observations (Tsimpidi et al., 2016). Nevertheless, SOA was still underpredicted during winter (NMB=-76%) indicating that other processes (e.g., seasonally dependent emissions and alternative oxidation paths) are a main cause of the inadequate performance.

Our results indicate that IVOCs can be major contributors to OA formation on a global scale. However, their abundance and physicochemical properties are poorly known, and more research is needed to determine the parameters that control their emissions, chemistry, and atmospheric removal. According to the model results, a combination of increased IVOC emissions, enhanced photochemical aging of IVOCs, and decreased hygroscopicity of the freshly emitted IVOCs can help reduce discrepancies between simulated SOA and observed OOA concentrations.

9. Acknowledgements

A.P. Tsimpidi acknowledges support from a DFG individual grand programme (project reference TS 335/2-1) and V.A. Karydis acknowledges support from a FP7 Marie Curie Career Integration Grant (project reference 618349).

Atmos. Chem. Phys. Discuss., doi:10.5194/acp-2017-6, 2017
Manuscript under review for journal Atmos. Chem. Phys.
Published: 11 January 2017

10. References

Aiken, A. C., Decarlo, P. F., Kroll, J. H., Worsnop, D. R., Huffman, J. A., Docherty, K. S., Ulbrich, I. M., Mohr, C., Kimmel, J. R., Sueper, D., Sun, Y., Zhang, Q., Trimborn, A., Northway, M., Ziemann, P. J., Canagaratna, M. R., Onasch, T. B., Alfarra, M. R., Prevot, A. S. H., Dommen, J., Duplissy, J., Metzger, A., Baltensperger, U., and Jimenez, J. L.: O/C and OM/OC ratios of primary, secondary, and ambient organic aerosols with high-resolution time-of-flight aerosol mass spectrometry, Environmen. Sci. & Technol., 42, 4478-4485, 2008.

Athanasopoulou, E., Vogel, H., Vogel, B., Tsimpidi, A. P., Pandis, S. N., Knote, C., and Fountoukis, C.: Modeling the meteorological and chemical effects of secondary organic aerosols during an EUCAARI campaign, Atmos. Chem. Phys., 13, 625-645, 2013.

Atkinson, R. and Arey, J.: Atmospheric degradation of volatile organic compounds, Chemical Reviews, 103, 4605-4638, 2003.

Bergstrom, R., van der Gon, H. A. C. D., Prevot, A. S. H., Yttri, K. E., and Simpson, D.: Modelling of organic aerosols over Europe (2002-2007) using a volatility basis set (VBS) framework: application of different assumptions regarding the formation of secondary organic aerosol, Atmos. Chem. Phys., 12, 8499-8527, 2012.

Canagaratna, M. R., Jimenez, J. L., Kroll, J. H., Chen, Q., Kessler, S. H., Massoli, P., Ruiz, L. H., Fortner, E., Williams, L. R., Wilson, K. R., Surratt, J. D., Donahue, N. M., Jayne, J. T., and Worsnop, D. R.: Elemental ratio measurements of organic compounds using aerosol mass spectrometry: characterization, improved calibration, and implications, Atmospheric Chemistry and Physics, 15, 253-272, 2015.

Chacon-Madrid, H. J., Henry, K. M., and Donahue, N. M.: Photo-oxidation of pinonaldehyde at low NOx: from chemistry to organic aerosol formation, Atmospheric Chemistry and Physics, 13, 3227-3236, 2013.

Clarke, L., Edmonds, J., Jacoby, H., Pitcher, H., Reilly, J., and Richels, R.: Scenarios of greenhouse gas emissions and atmospheric concentrations (Part A) and review of integrated scenario development and application (Part B). A report by the U.S. climate change science program and the subcommittee on global change research, 2007. 2007.

Donahue, N. M., Robinson, A. L., Stanier, C. O., and Pandis, S. N.: Coupled partitioning, dilution, and chemical aging of semivolatile organics, Environ. Sci. Technol., 40, 2635-2643, 2006.

Fountoukis, C., Megaritis, A. G., Skyllakou, K., Charalampidis, P. E., Pilinis, C., Denier van der Gon, H. A. C., Crippa, M., Canonaco, F., Mohr, C., Prévôt, A. S. H., Allan, J. D., Poulain, L., Petäjä, T., Tiitta, P., Carbone, S., Kiendler-Scharr, A., Nemitz, E., O'Dowd, C., Swietlicki, E., and Pandis, S. N.: Organic aerosol concentration and composition over Europe: insights from comparison of regional model predictions with aerosol mass spectrometer factor analysis, Atmos. Chem. Phys. Discuss., 14, 7597-7635, 2014.

Fountoukis, C., Racherla, P. N., van der Gon, H. A. C. D., Polymeneas, P., Charalampidis, P. E., Pilinis, C., Wiedensohler, A., Dall'Osto, M., O'Dowd, C., and Pandis, S. N.: Evaluation of a three-dimensional chemical transport model (PMCAMx) in the European domain during the EUCAARI May 2008 campaign, Atmos. Chem. and Phys., 11, 10331-10347, 2011.

Grieshop, A. P., Logue, J. M., Donahue, N. M., and Robinson, A. L.: Laboratory investigation of photochemical oxidation of organic aerosol from wood fires 1:

753 measurement and simulation of organic aerosol evolution, Atmos. Chem. Phys., 9,
754 1263-1277, 2009.
755 Hodzic, A., Aumont, B., Knote, C., Lee-Taylor, J., Madronich, S., and Tyndall, G.:
756 Volatility dependence of Henry's law constants of condensable organics:
757 Application to estimate depositional loss of secondary organic aerosols,
758 Geophysical Research Letters, 41, 4795-4804, 2014.
759 Hodzic, A., Jimenez, J. L., Madronich, S., Canagaratna, M. R., DeCarlo, P. F.,
760 Kleinman, L., and Fast, J.: Modeling organic aerosols in a megacity: potential
761 contribution of semi-volatile and intermediate volatility primary organic
762 compounds to secondary organic aerosol formation, Atmos. Chem. Phys., 10,
763 5491-5514, 2010.
764 Jathar, S. H., Farina, S. C., Robinson, A. L., and Adams, P. J.: The influence of semi-
765 volatile and reactive primary emissions on the abundance and properties of global
766 organic aerosol, Atmos. Chem. Phys., 11, 7727-7746, 2011.
767 Jathar, S. H., Gordon, T. D., Hennigan, C. J., Pye, H. O. T., Pouliot, G., Adams, P. J.,
768 Donahue, N. M., and Robinson, A. L.: Unspeciated organic emissions from
769 combustion sources and their influence on the secondary organic aerosol budget in
770 the United States, Proceedings of the National Academy of Sciences of the United
771 States of America, 111, 10473-10478, 2014.
772 Jathar, S. H., Miracolo, M. A., Presto, A. A., Donahue, N. M., Adams, P. J., and
773 Robinson, A. L.: Modeling the formation and properties of traditional and non-
774 traditional secondary organic aerosol: problem formulation and application to
775 aircraft exhaust, Atmospheric Chemistry and Physics, 12, 9025-9040, 2012.
776 Jimenez, J. L., Canagaratna, M. R., Donahue, N. M., Prevot, A. S. H., Zhang, Q.,
777 Kroll, J. H., DeCarlo, P. F., Allan, J. D., Coe, H., Ng, N. L., Aiken, A. C.,
778 Docherty, K. S., Ulbrich, I. M., Grieshop, A. P., Robinson, A. L., Duplissy, J.,
779 Smith, J. D., Wilson, K. R., Lanz, V. A., Hueglin, C., Sun, Y. L., Tian, J.,
780 Laaksonen, A., Raatikainen, T., Rautiainen, J., Vaattovaara, P., Ehn, M., Kulmala,
781 M., Tomlinson, J. M., Collins, D. R., Cubison, M. J., Dunlea, E. J., Huffman, J. A.,
782 Onasch, T. B., Alfarra, M. R., Williams, P. I., Bower, K., Kondo, Y., Schneider, J.,
783 Drewnick, F., Borrmann, S., Weimer, S., Demerjian, K., Salcedo, D., Cottrell, L.,
784 Griffin, R., Takami, A., Miyoshi, T., Hatakeyama, S., Shimono, A., Sun, J. Y.,
785 Zhang, Y. M., Dzepina, K., Kimmel, J. R., Sueper, D., Jayne, J. T., Herndon, S. C.,
786 Trimborn, A. M., Williams, L. R., Wood, E. C., Middlebrook, A. M., Kolb, C. E.,
787 Baltensperger, U., and Worsnop, D. R.: Evolution of organic aerosols in the
788 atmosphere, Science, 326, 1525-1529, 2009.
789 Jöckel, P., Tost, H., Pozzer, A., Bruehl, C., Buchholz, J., Ganzeveld, L., Hoor, P.,
790 Kerkweg, A., Lawrence, M. G., Sander, R., Steil, B., Stiller, G., Tanarhte, M.,
791 Taraborrelli, D., Van Aardenne, J., and Lelieveld, J.: The atmospheric chemistry
792 general circulation model ECHAM5/MESSy1: consistent simulation of ozone from
793 the surface to the mesosphere, Atmos. Chem. Phys., 6, 5067-5104, 2006.
794 Kanakidou, M., Seinfeld, J. H., Pandis, S. N., Barnes, I., Dentener, F. J., Facchini, M.
795 C., Van Dingenen, R., Ervens, B., Nenes, A., Nielsen, C. J., Swietlicki, E., Putaud,
796 J. P., Balkanski, Y., Fuzzi, S., Horth, J., Moortgat, G. K., Winterhalter, R., Myhre,
797 C. E. L., Tsigaridis, K., Vignati, E., Stephanou, E. G., and Wilson, J.: Organic
798 aerosol and global climate modelling: a review, Atmos. Chem. Phys., 5, 1053-
799 1123, 2005.
800 Kerkweg, A., Buchholz, J., Ganzeveld, L., Pozzer, A., Tost, H., and Jöckel, P.:
801 Technical Note: An implementation of the dry removal processes DRY DEPosition

and SEDImentation in the Modular Earth Submodel System (MESSy), Atmos. Chem. Phys., 6, 4617-4632, 2006a.

Kerkweg, A., Sander, R., Tost, H., and Jöckel, P.: Technical note: Implementation of prescribed (OFFLEM), calculated (ONLEM), and pseudo-emissions (TNUDGE) of chemical species in the Modular Earth Submodel System (MESSy), Atmos. Chem. Phys., 6, 3603-3609, 2006b.

Kroll, J. H. and Seinfeld, J. H.: Chemistry of secondary organic aerosol: Formation and evolution of low-volatility organics in the atmosphere, Atmos. Environ., 42, 3593-3624, 2008.

Lauer, A., Eyring, V., Hendricks, J., Joeckel, P., and Lohmann, U.: Global model simulations of the impact of ocean-going ships on aerosols, clouds, and the radiation budget, Atmos. Chem. Phys., 7, 5061-5079, 2007.

Li, G., Zavala, M., Lei, W., Tsimpidi, A. P., Karydis, V. A., Pandis, S. N., Canagaratna, M. R., and Molina, L. T.: Simulations of organic aerosol concentrations in Mexico City using the WRF-CHEM model during the MCMA-2006/MILAGRO campaign, Atmospheric Chemistry and Physics, 11, 3789-3809, 2011.

May, A. A., Levin, E. J. T., Hennigan, C. J., Riipinen, I., Lee, T., Collett, J. L., Jimenez, J. L., Kreidenweis, S. M., and Robinson, A. L.: Gas-particle partitioning of primary organic aerosol emissions: 3. Biomass burning, Journal of Geophysical Research-Atmospheres, 118, 11327-11338, 2013a.

May, A. A., Presto, A. A., Hennigan, C. J., Nguyen, N. T., Gordon, T. D., and Robinson, A. L.: Gas-particle partitioning of primary organic aerosol emissions: (1) Gasoline vehicle exhaust, Atmospheric Environment, 77, 128-139, 2013b.

May, A. A., Presto, A. A., Hennigan, C. J., Nguyen, N. T., Gordon, T. D., and Robinson, A. L.: Gas-Particle Partitioning of Primary Organic Aerosol Emissions: (2) Diesel Vehicles, Environmental Science & Technology, 47, 8288-8296, 2013c.

Murphy, B. N. and Pandis, S. N.: Simulating the formation of semivolatile primary and secondary organic aerosol in a regional chemical transport model, Environ. Sci. Technol., 43, 4722-4728, 2009.

Ots, R., Young, D. E., Vieno, M., Xu, L., Dunmore, R. E., Allan, J. D., Coe, H., Williams, L. R., Herndon, S. C., Ng, N. L., Hamilton, J. F., Bergström, R., Di Marco, C., Nemitz, E., Mackenzie, I. A., Kuenen, J. J. P., Green, D. C., Reis, S., and Heal, M. R.: Simulating secondary organic aerosol from missing diesel-related intermediate-volatility organic compound emissions during the Clean Air for London (ClearfLo) campaign, Atmos. Chem. Phys. Discuss., 2016, 1-36, 2016.

Pringle, K. J., Tost, H., Message, S., Steil, B., Giannadaki, D., Nenes, A., Fountoukis, C., Stier, P., Vignati, E., and Leieved, J.: Description and evaluation of GMXe: a new aerosol submodel for global simulations (v1), Geoscientific Model Development, 3, 391-412, 2010.

Pye, H. O. T. and Seinfeld, J. H.: A global perspective on aerosol from low-volatility organic compounds, Atmos. Chem. Phys., 10, 4377-4401, 2010.

Robinson, A. L., Donahue, N. M., Shrivastava, M. K., Weitkamp, E. A., Sage, A. M., Grieshop, A. P., Lane, T. E., Pierce, J. R., and Pandis, S. N.: Rethinking organic aerosols: Semivolatile emissions and photochemical aging, Science, 315, 1259-1262, 2007.

Robinson, A. L., Grieshop, A. P., Donahue, N. M., and Hunt, S. W.: Updating the conceptual model for fine particle mass emissions from combustion systems, J. Air Waste Manage., 60, 1204-1222, 2010.

Atmos. Chem. Phys. Discuss., doi:10.5194/acp-2017-6, 2017
Manuscript under review for journal Atmos. Chem. Phys.
Published: 11 January 2017

Atmospheric Chemistry and Physics Discussions

851 Sander, R., Baumgaertner, A., Gromov, S., Harder, H., Joeckel, P., Kerkweg, A.,
852 Kubistin, D., Regelin, E., Riede, H., Sandu, A., Taraborrelli, D., Tost, H., and Xie,
853 Z. Q.: The atmospheric chemistry box model CAABA/MECCA-3.0, Geoscientific
854 Model Development, 4, 373-380, 2011.
855 Shrivastava, M., Fast, J., Easter, R., Gustafson, W. I., Jr., Zaveri, R. A., Jimenez, J. L.,
856 Saide, P., and Hodzic, A.: Modeling organic aerosols in a megacity: comparison of
857 simple and complex representations of the volatility basis set approach, Atmos.
858 Chem. Phys., 11, 6639-6662, 2011.
859 Shrivastava, M. K., Lane, T. E., Donahue, N. M., Pandis, S. N., and Robinson, A. L.:
860 Effects of gas particle partitioning and aging of primary emissions on urban and
861 regional organic aerosol concentrations, J. Geophys. Res.-Atmos., 113, 2008.
862 Tost, H., Jöckel, P., Kerkweg, A., Sander, R., and Lelieveld, J.: Technical note: A
863 new comprehensive SCAVenging submodel for global atmospheric chemistry
864 modelling, Atmos. Chem. Phys., 6, 565-574, 2006.
865 Tsimpidi, A. P., Karydis, V. A., Pandis, S. N., and Lelieveld, J.: Global combustion
866 sources of organic aerosols: Model comparison with 84 AMS factor analysis data
867 sets, Atmos. Chem. Phys. Discuss., 2016, 1-51, 2016.
868 Tsimpidi, A. P., Karydis, V. A., Pozzer, A., Pandis, S. N., and Lelieveld, J.: ORACLE
869 (v1.0): module to simulate the organic aerosol composition and evolution in the
870 atmosphere, Geoscientific Model Development, 7, 3153-3172, 2014.
871 Tsimpidi, A. P., Karydis, V. A., Zavala, M., Lei, W., Bei, N., Molina, L., and Pandis,
872 S. N.: Sources and production of organic aerosol in Mexico City: insights from the
873 combination of a chemical transport model (PMCAMx-2008) and measurements
874 during MILAGRO, Atmos. Chem. Phys., 11, 5153-5168, 2011.
875 Tsimpidi, A. P., Karydis, V. A., Zavala, M., Lei, W., Molina, L., Ulbrich, I. M.,
876 Jimenez, J. L., and Pandis, S. N.: Evaluation of the volatility basis-set approach for
877 the simulation of organic aerosol formation in the Mexico City metropolitan area,
878 Atmos. Chem. Phys., 10, 525-546, 2010.
879 van der Werf, G. R., Randerson, J. T., Giglio, L., Collatz, G. J., Mu, M., Kasibhatla,
880 P. S., Morton, D. C., DeFries, R. S., Jin, Y., and van Leeuwen, T. T.: Global fire
881 emissions and the contribution of deforestation, savanna, forest, agricultural, and
882 peat fires (1997-2009), Atmos. Chem. Phys., 10, 11707-11735, 2010.
883 Zhang, Q. J., Beekmann, M., Drewnick, F., Freutel, F., Schneider, J., Crippa, M.,
884 Prevot, A. S. H., Baltensperger, U., Poulain, L., Wiedensohler, A., Sciare, J., Gros,
885 V., Borbon, A., Colomb, A., Michoud, V., Doussin, J. F., van der Gon, H. A. C.
886 D., Haeffelin, M., Dupont, J. C., Siour, G., Petetin, H., Bessagnet, B., Pandis, S.
887 N., Hodzic, A., Sanchez, O., Honore, C., and Perrussel, O.: Formation of organic
888 aerosol in the Paris region during the MEGAPOLI summer campaign: evaluation
889 of the volatility-basis-set approach within the CHIMERE model, Atmos. Chem.
890 Phys., 13, 5767-5790, 2013.

891

892

Atmos. Chem. Phys. Discuss., doi:10.5194/acp-2017-6, 2017
Manuscript under review for journal Atmos. Chem. Phys.
Published: 11 January 2017

Atmospheric Chemistry and Physics Discussions

893

894 **Table 1.** Parameters used in the sensitivity simulations

895

Simulation	**Emission factor**		**Emission rate** (Tg yr^{-1})		**Volatility bins**	**Reduction in volatility** (μg m^{-3})	**Stoichiometric coefficient of aging reactions**	**Oxidation rate constant** (cm^3 $molec^{-1}$ s^{-1})	**Henry's law constant** (mol $L^{-1}atm^{-1}$)	
	fPOA	bbPOA	fPOA	bbPOA					Freshly emitted	Aged
Reference	2.5	1	44.2	28.4	5	10^2	1.15	$2x10^{-11}$	10^5	10^5
Low volatility	1	1	17.7	28.4	5	10^2	1.15	$2x10^{-11}$	10^5	10^5
High IVOCs	4	2.5	70.7	71	5	10^2	1.15	$2x10^{-11}$	10^5	10^5
Alternative POA emissions	2.5	1	28.5	37.8	5	10^2	1.15	$2x10^{-11}$	10^5	10^5
High reaction rate constant	2.5	1	44.2	28.4	5	10^2	1.15	$4x10^{-11}$	10^5	10^5
Alternative aging scheme	2.5	1	44.2	28.4	9	10	1.075	$4x10^{-11}$	10^5	10^5
Hybrid aging scheme	2.5	1	44.2	28.4	5	SVOCs:10^2 IVOCs:10^4-10^6	SVOCs:1.15 IVOCs:1.115-0.71	SVOCs:$2x10^{-11}$ IVOCs:$1.2x10^{-11}$	10^5	10^5
Low solubility	2.5	1	44.2	28.4	5	10^2	1.15	$2x10^{-11}$	10^3	10^3
Variable solubility	2.5	1	44.2	28.4	5	10^2	1.15	$2x10^{-11}$	10	10^5

Atmos. Chem. Phys. Discuss., doi:10.5194/acp-2017-6, 2017
Manuscript under review for journal Atmos. Chem. Phys.
Published: 11 January 2017

Atmospheric Chemistry and Physics Discussions

896 **Table 2.** Statistical evaluation of EMAC POA (sum of fPOA and bbPOA) against
897 AMS POA (sum of HOA and BBOA) using 61 data sets in urban downwind and rural
898 areas during 2001-2010.
899

Simulation Name	**Mean Observed** (μg m^{-3})	**Mean Predicted** (μg m^{-3})	**MAGE** (μg m^{-3})	**MB** (μg m^{-3})	**NME** (%)	**NMB** (%)	**RMSE** (μg m^{-3})
Reference	0.53	0.51	0.38	-0.02	71	-3	0.50
Low volatility		0.75	0.46	0.22	88	43	0.64
High IVOCs		0.52	0.38	-0.01	73	0	0.51
Alternative POA emissions		0.39	0.33	-0.14	63	-25	0.44
High reaction rate constant		0.50	0.37	-0.03	70	-5	0.49
Conservative aging scheme		0.17	0.42	-0.36	79	-67	0.60
Hybrid aging scheme		0.50	0.38	-0.03	72	-4	0.50
Low solubility		0.53	0.38	0	72	1	0.50
Variable solubility		0.54	0.38	0.01	73	4	0.51

900
901

Atmos. Chem. Phys. Discuss., doi:10.5194/acp-2017-6, 2017
Manuscript under review for journal Atmos. Chem. Phys.
Published: 11 January 2017

Atmospheric Chemistry and Physics Discussions

902 **Table 3.** Statistical evaluation of EMAC SOA against AMS OOA using 61 data sets
903 in downwind urban and rural areas during 2001-2010.
904

Simulation Name	Mean Observed (μg m^{-3})	Mean Predicted (μg m^{-3})	MAGE (μg m^{-3})	MB (μg m^{-3})	NME (%)	NMB (%)	RMSE (μg m^{-3})
Reference	2.78	1.91	1.39	-0.87	50	-31	2.02
Low volatility		1.32	1.69	-1.46	61	-52	2.30
High IVOCs		2.50	1.47	-0.28	53	-10	2.05
Alternative POA emissions		1.66	1.55	-1.12	56	-40	2.15
High reaction rate constant		2.16	1.32	-0.62	48	-22	1.97
Conservative aging scheme		1.73	1.49	-1.05	53	-38	2.09
Hybrid aging scheme		1.71	1.46	-1.08	53	-39	2.08
Low solubility		2.10	1.33	-0.68	48	-25	1.98
Variable solubility		2.14	1.32	-0.64	48	-23	1.97

905
906

Atmos. Chem. Phys. Discuss., doi:10.5194/acp-2017-6, 2017
Manuscript under review for journal Atmos. Chem. Phys.
Published: 11 January 2017

Atmospheric Chemistry and Physics Discussions

907 **Table 4.** Percentage change of the tropospheric burden of organic aerosol components for
908 each sensitivity simulation relative to the reference simulation during the decade 2001-2010.
909 Positive change corresponds to an increase. The predicted tropospheric burden in Tg of the
910 reference simulation is also shown.

	fPOA	bbPOA	fSOA-sv	bbSOA-sv	fSOA-iv	bbSOA-iv	Total OA
Tropospheric burden of reference (Tg)	0.06	0.18	0.13	0.21	0.44	0.2	1.98
	Percentage Change (%) from reference						
Simulation Name							
Low volatility	53	48	14	39	-100	-100	-23
High IVOCs	7	5	-3	-4	88	165	38
Alternative POA emissions	-39	10	-33	11	-34	11	-8
High reaction rate constant	-10	-7	11	11	8	6	4
Alternative aging scheme	-65	-38	-68	-47	14	30	-10
Hybrid aging scheme	-2	-1	2	2	-37	-36	-13
Low solubility	6	1	11	4	21	8	8
Variable solubility	9	2	14	5	22	7	8

911
912
913
914
915
916
917
918

Atmos. Chem. Phys. Discuss., doi:10.5194/acp-2017-6, 2017
Manuscript under review for journal Atmos. Chem. Phys.
Published: 11 January 2017

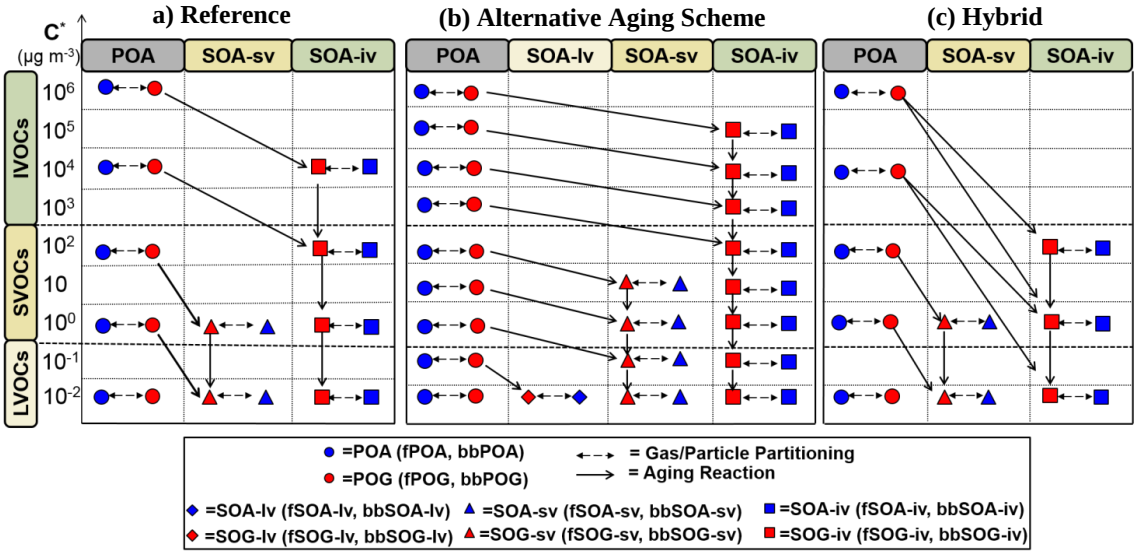

Figure 1: Schematic of the VBS resolution and the formation of SOA from SVOCs and IVOCs in the: (a) reference simulation, (b) alternative aging scheme and (c) hybrid case. SOA from LVOCs (SOA-lv) is only formed in the alternative aging scheme (b). Red indicates that the organic compound is in the vapor phase and blue in the particulate phase. The circles correspond to primary organics emitted as gases or particles. Diamonds symbolize the formation of SOA from LVOC emissions by fuel combustion and biomass burning. Triangles indicate SOA formation from SVOC emissions by fuel combustion and biomass burning, while the squares show SOA from IVOC by the same sources. Gas-aerosol partitioning, aging reactions, and names of species are also shown.

Atmos. Chem. Phys. Discuss., doi:10.5194/acp-2017-6, 2017
Manuscript under review for journal Atmos. Chem. Phys.
Published: 11 January 2017

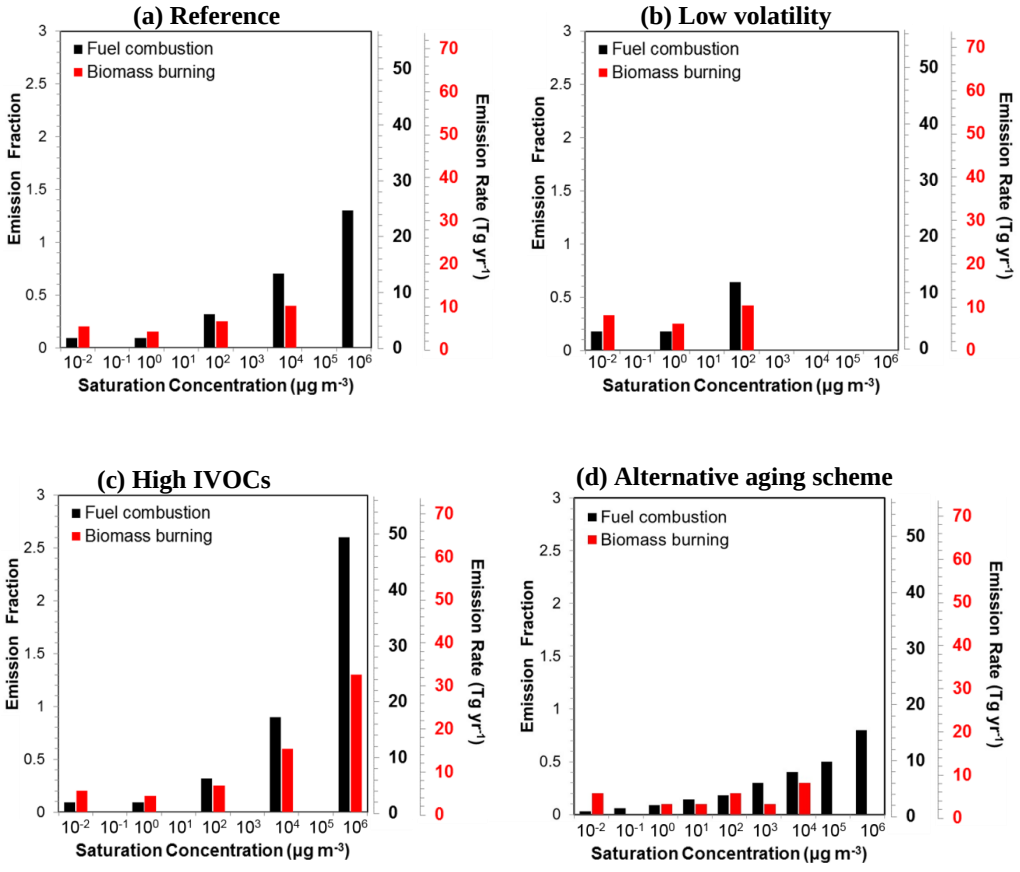

Figure 2. Volatility distribution for fuel combustion (black) and biomass burning OA (red) for the (a) reference, (b) low volatility, (c) high IVOCs and (d) conservative aging scheme simulations. The reference emission factors are from Robinson et al. (2007) for fPOA and May et al. (2013) for bbPOA emissions. The emission rates of fPOA and bbPOA are also shown on the right axis.

Atmos. Chem. Phys. Discuss., doi:10.5194/acp-2017-6, 2017
Manuscript under review for journal Atmos. Chem. Phys.
Published: 11 January 2017

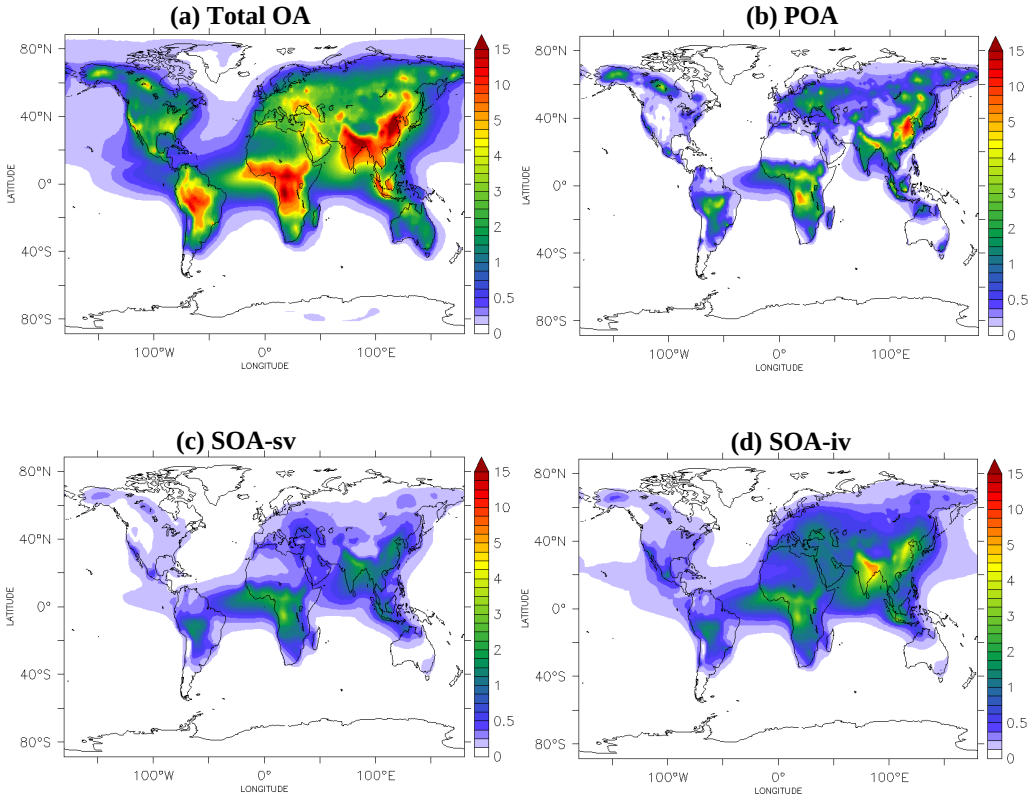

Figure 3: Predicted average surface concentrations (in μg m^{-3}) of: **(a)** Total OA (sum of POA, SOA-sv, SOA-iv and SOA-v), **(b)** POA and **(c)** SOA from the oxidation of SVOCs (SOA-sv) and **(d)** SOA from the oxidation of IVOCs (SOA-iv) for the reference simulation during the 2001-2010 period.

Atmos. Chem. Phys. Discuss., doi:10.5194/acp-2017-6, 2017
Manuscript under review for journal Atmos. Chem. Phys.
Published: 11 January 2017

Atmospheric Chemistry and Physics Discussions

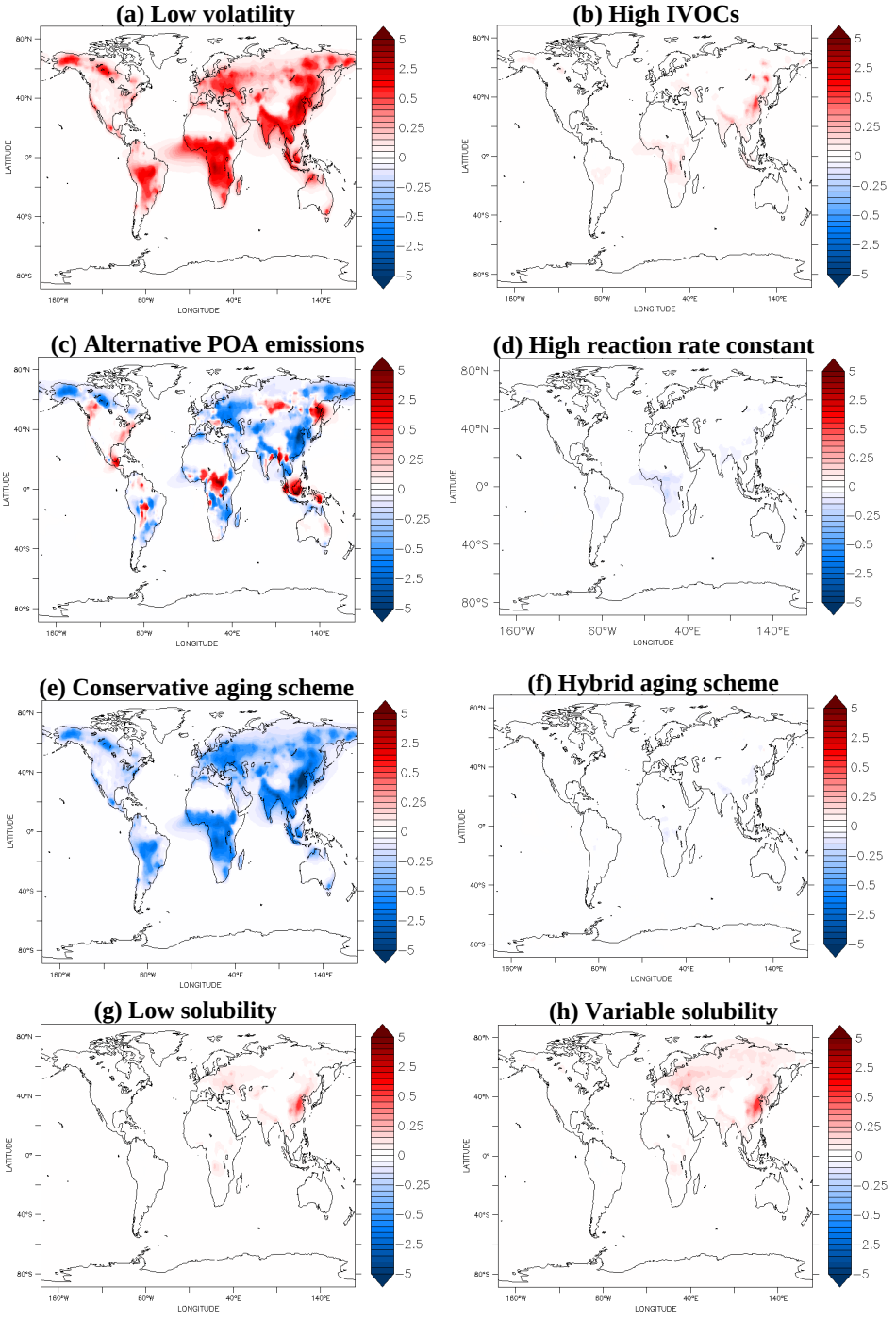

1000

Figure 4: Absolute changes (in μg m^{-3}) of the average surface POA concentrations between the reference and the **(a)** low volatility, **(b)** high IVOCs, **(c)** alternative POA emissions, **(d)** high reaction rate constant, **(e)** conservative aging scheme, **(f)** hybrid aging scheme, **(g)** low solubility, and, **(h)** hybrid solubility simulations during the period 2001-2010. A positive change indicates an increase in the sensitivity test.

Atmos. Chem. Phys. Discuss., doi:10.5194/acp-2017-6, 2017
Manuscript under review for journal Atmos. Chem. Phys.
Published: 11 January 2017

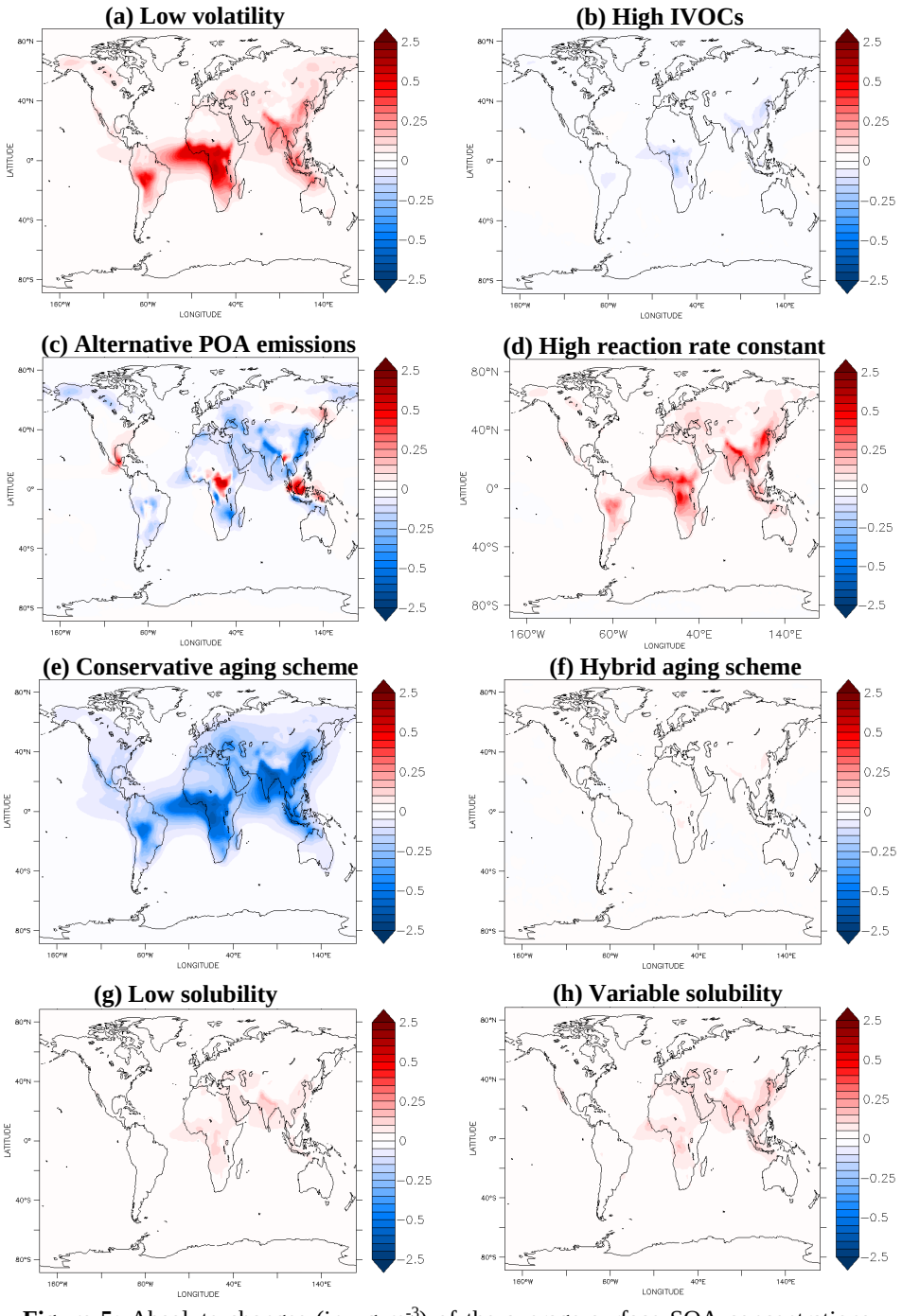

Figure 5: Absolute changes (in μg m^{-3}) of the average surface SOA concentrations from SVOCs (SOA-sv) between the reference and the **(a)** low volatility, **(b)** high IVOCs, **(c)** alternative POA emissions, **(d)** high reaction rate constant, **(e)** conservative aging scheme, **(f)** hybrid aging scheme, **(g)** low solubility, and, **(h)** hybrid solubility simulations during the period 2001-2010. A positive change indicates an increase in the sensitivity test.

Atmos. Chem. Phys. Discuss., doi:10.5194/acp-2017-6, 2017
Manuscript under review for journal Atmos. Chem. Phys.
Published: 11 January 2017

Atmospheric Chemistry and Physics Discussions

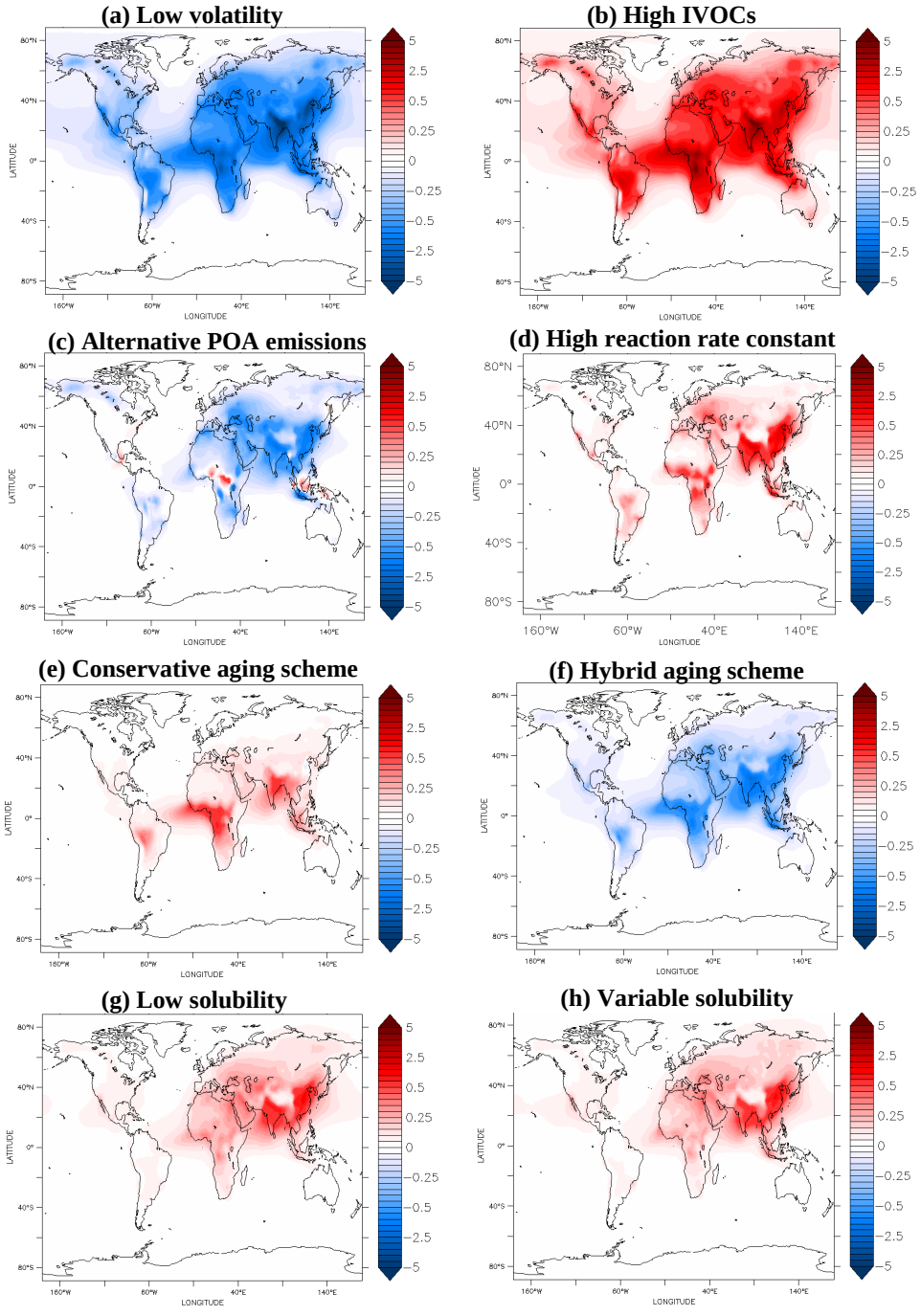

Figure 6: Absolute changes (in μg m^{-3}) of the average surface SOA concentrations from IVOCs (SOA-iv) between the reference and the **(a)** low volatility, **(b)** high IVOCs, **(c)** alternative POA emissions, **(d)** high reaction rate constant, **(e)** conservative aging scheme, **(f)** hybrid aging scheme, **(g)** low solubility, and, **(h)** hybrid solubility simulations during the period 2001-2010. A positive change indicates an increase in the sensitivity test.

Atmos. Chem. Phys. Discuss., doi:10.5194/acp-2017-6, 2017
Manuscript under review for journal Atmos. Chem. Phys.
Published: 11 January 2017

Atmospheric Chemistry and Physics Discussions

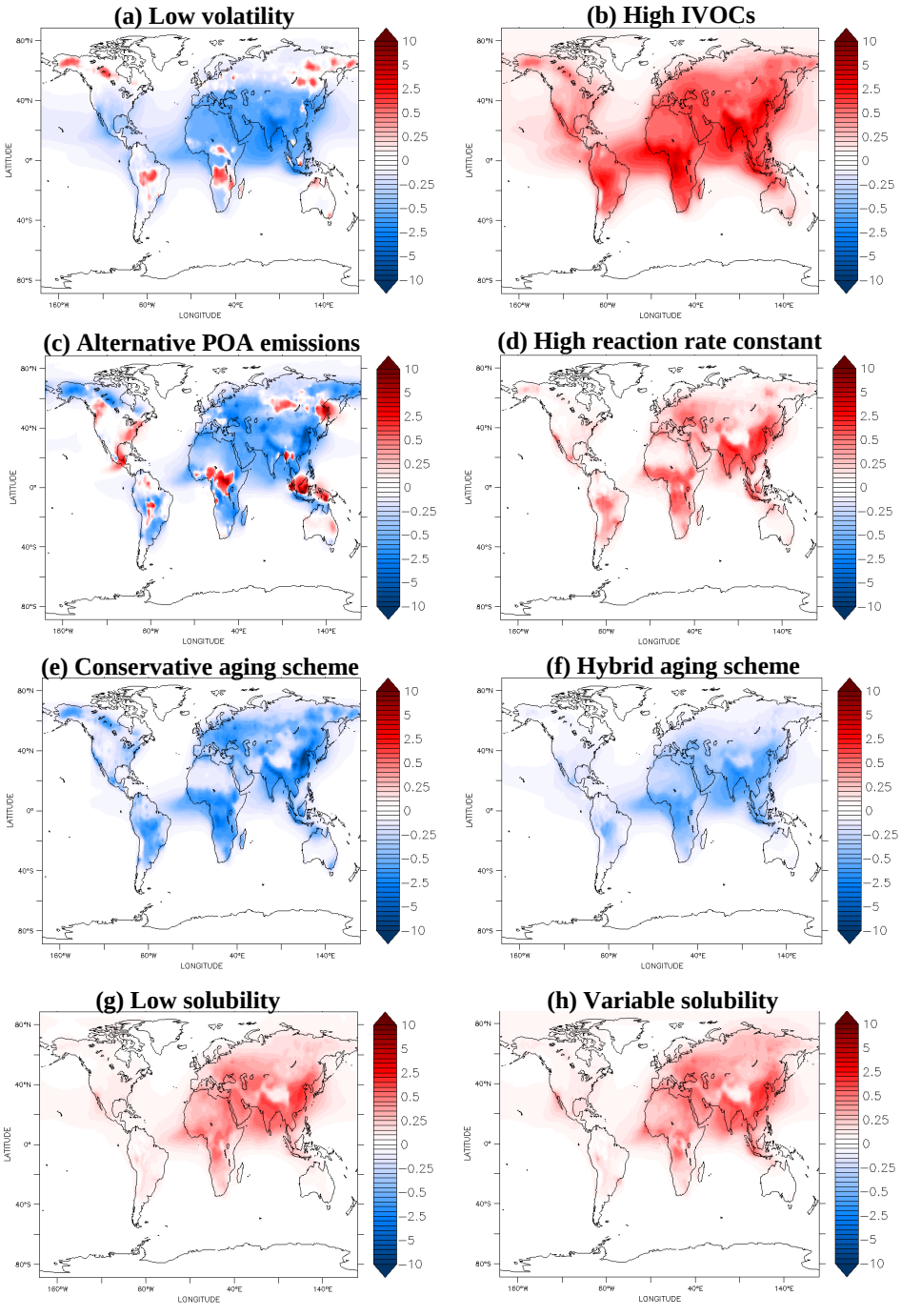

1100

Figure 7: Absolute changes (in μg m^{-3}) of the average surface total OA concentrations between the reference and the **(a)** low volatility, **(b)** high IVOCs, **(c)** alternative POA emissions, **(d)** high reaction rate constant, **(e)** conservative aging scheme, **(f)** hybrid aging scheme, **(g)** low solubility, and, **(h)** hybrid solubility simulations during the period 2001-2010. A positive change indicates an increase in the sensitivity test.

Atmos. Chem. Phys. Discuss., doi:10.5194/acp-2017-6, 2017
Manuscript under review for journal Atmos. Chem. Phys.
Published: 11 January 2017

Atmospheric Chemistry and Physics Discussions

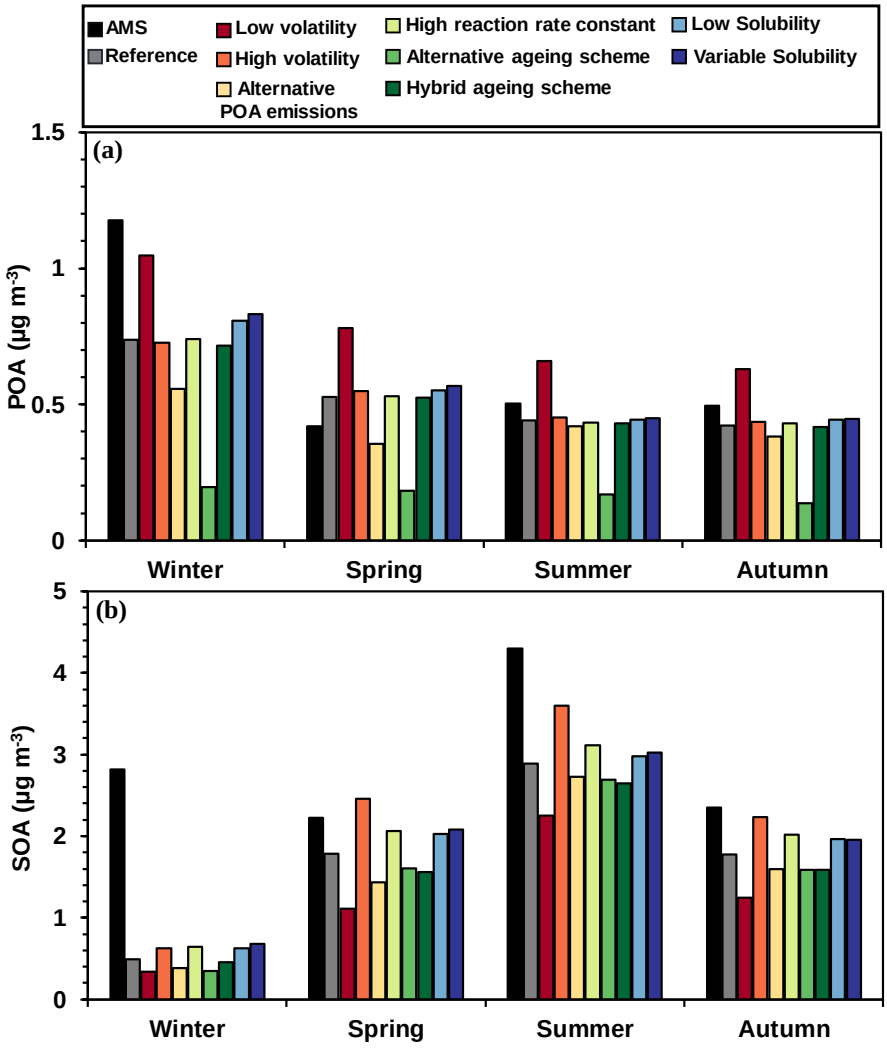

Figure 8: Average (a) POA and (b) SOA concentrations (in µg m^{-3}) measured and predicted in the reference and sensitivity simulations during winter, spring, summer, and autumn in urban-downwind and rural areas of the continental Northern Hemisphere.